Hop-by-Hop ZF Beamforming for MIMO Full-Duplex Relaying With Co-Channel Interference

Ahmed Almradi, Pei Xiao, *Senior Member, IEEE*, and Khairi Ashour Hamdi, *Senior Member, IEEE*

***Abstract*— In this paper, a comprehensive design and analysis of multiple-input multiple-output (MIMO) full-duplex (FD) relaying systems in a multi-cell environment is investigated, where a multi-antenna amplify-and-forward FD relay station serves multiple half-duplex (HD) multi-antenna users. The pivotal obstacles of loopback self-interference (LI) and multiple co-channel interferers (CCI) at the relay and destination when employing FD relaying in cellular networks are addressed. In contrast to the HD relaying mode, the CCI in the FD relaying mode is predicted to double since the uplink and downlink communications are simultaneously scheduled via the same channel. In this paper, the optimal layout of transmit (receive) precoding (decoding) weight vectors which maximizes the overall signal-to-interference-plus-noise ratio is constructed by a suitable optimization problem, and then a closed-form sub-optimal formula based on null space projection is presented. The proposed hop-by-hop rank-1 zero-forcing (ZF) beamforming vectors are based on added ZF constraints used to suppress the LI and CCI channels at the relay and destination, i.e., the source and relay perform transmit ZF beamforming, while the relay and destination employ receive ZF combining. To this end, unified accurate expressions for the outage probability and ergodic capacity are derived in closed form. In addition, simpler tight lower bound formulas for the outage probability and ergodic capacity are presented. Moreover, the asymptotic approximations for outage probability are considered to gain insights into system behavior in terms of the diversity order and array gain. Numerical and simulation results show the accuracy of the presented exact analytical expressions and the tightness of the lower bound expressions. The case of hop-by-hop maximum-ratio transmission/maximal-ratio combining beamforming is included for comparison purposes. Furthermore, our results show that while multi-antenna terminals improve the system performance, the detrimental effect of CCI on FD relaying is clearly seen. Therefore, our findings unveil that MIMO FD relaying could significantly improve the system performance compared to its conventional MIMO HD relaying counterpart.**

***Index Terms*— MIMO relaying, full-duplex relaying, half-duplex relaying, beamforming, zero-forcing (ZF), outage probability, ergodic capacity, co-channel interference.**

I. Introduction

TRADITIONAL dual-hop relaying networks and base stations operate in the half-duplex (HD) mode, thereby two orthogonal channels (i.e., in a time division duplex or frequency division duplex manner) are essential to initiate communications. Lately, full-duplex (FD) relaying received upsurge of research interest due to its capability to increase spectral efficiency (see e.g., [1]–[8]), which is solely because of the fact that full-duplex nodes receive and re-transmit the information symbol over the same time and frequency, consequently, efficiently employing the spectrum resources of the network. However, the main hurdle of FD terminals is the loopback self-interference (LI) brought about by the signal infiltration from the terminal's transmission to its own reception, specifically, the huge power differences between the one transmitted from the FD terminal and its received signal (the received signal is extremely weaker than that of the transmitted one due to the heavy path loss and fading), which surpass the dynamic range of the analoge-to-digital converter. Therefore, LI alleviation and elimination is indispensable for the implementation of FD mode operation [1]–[5], [9].

The explosive growth in demand for wireless communication devices with higher throughput (a principal merit of 5G wireless communication systems) led to the implementation of short range systems, such as small-cell networks, WiFi, and Femtocells, where the cell-edge path loss is lower than that of the traditional cellular networks. Therefore, the transmission power and distance between devices have been greatly reduced. This considerable amendment alongside the developments in antennas and radio-frequency (RF) circuit design render full-duplex communications feasible as the LI mitigation problem becomes viable. Various LI attenuation approaches have been proposed in the literature which may be classified into three phases: propagation (passive) domain LI cancelation, analog and digital (active) domain LI cancelation, and spatial domain LI cancelation (in the presence of multiple receive and/or transmit antennas at the FD node) [2], [4]–[12]. Owing to the significant hardware adjustment, high cost and

Manuscript received January 4, 2018; revised April 30, 2018 and June 29, 2018; accepted July 29, 2018. Date of publication August 6, 2018; date of current version December 14, 2018. This work was supported in part by the U.K. Engineering and Physical Sciences Research Council under Grant EP/N020391/1, and in part by the European Commission under the 5GPPP project 5GXcast (H2020-ICT-2016-2 call, grant number 761498). This paper was presented in part at the IEEE GLOBECOM, Washington DC, USA, December 2016. The associate editor coordinating the review of this paper and approving it for publication was W. Chen. *(Corresponding author: Ahmed Almradi.)*

A. Almradi and P. Xiao are with the 5G Innovation Centre, Institute for Communication Systems, University of Surrey, Guildford GU2 7XH, U.K. (e-mail: a.m.almradi@surrey.ac.uk; p.xiao@surrey.ac.uk).

K. A. Hamdi is with the School of Electrical and Electronic Engineering, The University of Manchester, Manchester M13 9PL, U.K. (e-mail: k.hamdi@manchester.ac.uk).

Color versions of one or more of the figures in this paper are available online at http://ieeexplore.ieee.org.

Digital Object Identifier 10.1109/TCOMM.2018.2863723

power required by the terminal to operate in the FD mode, only infrastructure base stations are upgraded to operate on the FD mode, while user terminals persist to operate in the HD mode.

Synergistic conjunction of multiple-input-multiple-output (MIMO) techniques with FD relaying systems delivers a new dimension of LI suppression in the spatial domain, and also can provide higher capacity in contrast to its HD relaying rival (see e.g., [7], [8], [10], [13]). Hence, when a FD relaying networks with multi-antenna terminals is present, joint optimization of precoding and decoding at the transmitter and receiver, respectively, can be utilized to diminish the LI impact at the relay. Owing to its deployment simplicity and analytical tractability, zero-forcing (ZF) technique is employed to totally nullify the LI interference and terminate the closed-loop between the relay input and output. Several papers have investigated the spatial LI alleviation issue, for instance, in [7] and [13], a new precoding and decoding vector design relies on the conventional singular value decomposition (SVD) of the LI channel is introduced to cancel out the LI at the relay, Riihonen *et al.* [7] further considered various spatial LI elimination methods, more specifically, the antenna selection, beam selection, and null space projection techniques have been studied. In addition, a joint beamforming and combining weights layout for the maximization of the overall signal-to-interefernce-plus-noise ratio (SINR) is investigated in [8], thereby a closed-form overall SINR is presented. Namely, the receive ZF precoding with maximum-ratio transmission (MRT), and the maximal-ratio combining (MRC) with transmit ZF schemes have been introduced. More recently, Ngo *et al.* [6] exploited the theory of massive MIMO at the receiver and the transmiter to greatly minimize the LI effect, where the ZF/ZF and MRC/MRT schemes are used at the decode-and-forward (DF) FD relay. In [10], several transmit and receive heuristic filters which maximizes the overall signal-to-noise ratio (SNR) for the MIMO FD relaying systems are presented. The null space projection via SVD is utilized by Tsimenidis and Rawi [14] to suppress the LI interference. Note that the SVD based approach in [7] and [14] is considered under specific assumptions on the number of relay receive and transmit antennas. However, to our best knowledge, the effect of co-channel interference (CCI)[1] on the overall performance of FD relaying with multiple-antenna terminals has not been investigated yet, i.e., the general case of multiple antenna terminals with CCI at the relay and destination, utilizing transmit (receive) ZF beamforming (combining) has not been analyzed in the literature for both HD and FD relaying modes.[2] Note that ZF beamforming is employed particularly due to its robustness against the severe effects of CCI and fading, where this is achieved by steering the transmitted signal along the strongest eigenmodes of the source $\rightarrow$ relay ($\boldsymbol{S} \rightarrow \boldsymbol{R}$) and relay $\rightarrow$ destination ($\boldsymbol{R} \rightarrow \boldsymbol{D}$) null-space-projected channels.

In the context of traditional HD relaying networks, the impact of CCI due to frequency reuse on the system performance has been extensively studied in the literature (see e.g., [15]–[22]). However, FD relaying networks are more susceptible to CCI because of the higher frequency reuse in contrast to its conventional HD relaying rival. For instance, in the case of multi-cell framework where FD relay base stations and HD users, an extremely greater level of CCI is noticed from nearby cells in comparison to the HD relaying networks [1], [23]–[25]. Therefore, it is of theoretical and practical significance to analyze the deleterious impact of CCI on the performance of FD relaying networks. Alves *et al.* [24] and Sharma *et al.* [25] investigated the effect of CCI on the performance of FD relaying networks, namely, the outage probability of a DF FD relay with single antenna nodes has been presented. In [23], the average spectral efficiency of a stochastic geometry small cell networks, when both the base stations and user equipments operate in FD mode (i.e., terminals have dedicated antennas for transmission and reception) is presented. Note that all these previous works are restricted to single antenna terminals. More recently, Almradi and Hamdi [26], [27] investigated the impact of CCI on the performance of MIMO FD relaying systems, where a single antenna terminals are considered. However, the implementation of multiple antenna terminals enhance reliability and improve capacity, further, it is a powerful approach that can be used to mitigate the LI and CCI effects at the relay and destination.

Inspired by the above stated limitations, this paper provides a thorough investigation for the impact of LI and CCI at the relay and destination on the performance of amplify-and-forward FD relaying networks with multi-antenna nodes by employing hop-by-hop ZF beamforming. Furthermore, the case of hop-by-hop MRT/MRC beamforming is also presented as a benchmark.

The major contributions of the paper are outlined as:

1) The design of precoding and decoding vectors which maximizes the overall SINR is formulated by proper optimization problem. Since the optimal precoding and decoding weight vectors do not yield a mathematically tractable overall SINR formula, a sub-optimal solution based on added ZF (null space projection) constraints is proposed.[3] The hop-by-hop ZF beamforming weight vectors are designed to suppress the CCI and LI at the FD relay, and the CCI at the destination as follows: the receive ZF combining filter at the relay is adjusted to terminate the CCI interferers at the relay, and the transmit ZF beamforming filter at the relay is intended

[1]The frequency reuse to improve the spectrum efficiency of wireless networks causes the harmful effect of CCI in the FD multi-cell environment.

[2]It is to be emphasized that the performance of MIMO half-duplex relaying systems with CCI at the relay and/or destination has been studied in [15]–[22]. However, all these system set-ups are limited to one or two single antenna terminals (except for [18] and [21]), resulting in a simplified analytical expressions. Meanwhile, [18] and [21] investigated the performance analysis of transmit antenna selection (TAS)/MRC and MRT/MRC, respectively. However, due to the presence of CCI, MRC and MRT are sub-optimal schemes as they treat the interference as additive noise. Therefore, this paper presents a more sophisticated null space projection scheme in order to suppress the CCI at the relay and destination.

[3]It is widely common that the ZF technique totally terminates the CCI and results in noise enhancement at low interference-to-noise ratio (INR). Meanwhile, minimum mean square error (MMSE) strikes a balance between CCI interference suppression and noise amplification. It should be noted that the ZF scheme is optimal in the high INR regime, i.e., the MMSE and ZF performances match at the asymptotically high INR regime.

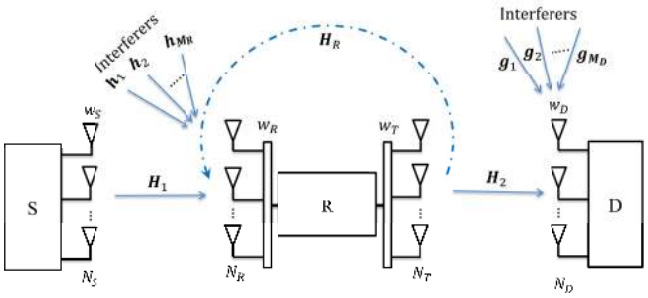

Fig. 1. The MIMO FD relaying system model.

to suppress the LI at the relay, while the receive ZF combining filter at the destination is aimed to cancel out the CCI interferers at the destination. Therefore, simple closed-form overall SINR expression is presented based on the derived closed-form transmit/receive ZF beamforming/combining vectors. Meanwhile, the hop-by-hop MRT/MRC beamforming scheme is introduced for comparison purposes.

2) A unified accurate closed-form formula for the outage probability of multi-antenna FD relaying networks with LI and CCI is presented, where hop-by-hop ZF beamforming is performed. In addition, a simple outage probability lower-bound expression is formulated in closed-form. Besides, the asymptotic behavior of the considered system is also included, and shown to achieve a diversity order of $\min\left(N_S\left(N_R-M_R\right),\left(N_T-1\right)\left(N_D-M_D\right)\right)$, where N_S and N_D are the number of antennas at the source and destination, N_T and N_R are the number of FD relay transmit and receive antennas, and M_R and M_D are the number of CCI interferers at the relay and destination, respectively.
3) A unified accurate closed-form ergodic capacity formula for the MIMO FD relaying systems with LI and CCI is derived, further, a simple ergodic capacity lower-bound formula is also included.

The layout of the remaining bit of this paper is as follows. In Sec. II, the system model is introduced. In Sec. III, we address the instantaneous overall SINR. In Sec. IV, we study the outage probability analysis. In Sec. V, the ergodic capacity analysis is presented. Numerical results are provided in Sec. VI. Finally, Sec. VII concludes the paper.

II. The System Model

We study a MIMO FD amplify-and-forward (AF) relaying system, where a source $\boldsymbol{S}$ with N_S transmitting antennas is communicating with a destination $\boldsymbol{D}$ having N_D receiving antennas through a multi-antenna FD relay $\boldsymbol{R}$ with N_R receiving antennas and N_T transmitting antennas, where the relay is subject to loopback self-interference (LI) and M_R co-channel interferers (CCI), while the destination is subject to M_D CCI as depicted in Fig. 1. Throughout this paper, the following assumptions are considered: 1) It is assumed that the source does not have a direct link to the destination due to heavy path loss and shadowing since the main focus of our work is on network coverage extension. 2) A single MIMO full-duplex AF relay station is considered with MIMO half-duplex users (i.e., HD source and destination), where the full-duplex relay receives and re-transmits its information at the same time over the same frequency. 3) Channels are modeled as quasi-static block flat fading and remain constant over the block time T, and varies independently and identically from one block to the next. The $\boldsymbol{S}\rightarrow\boldsymbol{R}$ channel is represented by $\boldsymbol{H}_1$ which is a $N_R\times N_S$ matrix, the $\boldsymbol{R}\rightarrow\boldsymbol{D}$ channel is represented by $\boldsymbol{H}_2$ which is a $N_D\times N_T$ matrix, the i^{th} interference channel at the FD node is denoted by $\boldsymbol{h}_i$ which is a $N_R\times 1$ vector, and the j^{th} interferer channel at the destination is denoted by $\boldsymbol{g}_j$ which is $N_D\times 1$ vector entries follow independent and identically distributed random variables ($i.\,i.\,d.$) and distributed according to $\mathcal{CN}\left(0,\,1\right)$, while the relay $\rightarrow$ relay ($\boldsymbol{R}\rightarrow\boldsymbol{R}$) residual LI channel is represented by $\boldsymbol{H}_R$ which is a $N_R\times N_T$ matrix, and represents the residual error by imperfect LI suppression deployed via the passive and active domain LI cancelation at the FD node, with entries follow $i.\,i.\,d.$ random variables and distributed according to $\mathcal{CN}\left(0,\,\sigma_R^2\right)$, where σ_R^2 reflects the amount of LI suppression. Perfect channel state information (CSI) of the $\boldsymbol{S}\rightarrow\boldsymbol{R}$ channel $\boldsymbol{H}_1$ and the i^{th} interferer channel $\boldsymbol{h}_i$ with $i=1,\,\ldots,\,M_R$ are assumed to be available at the source and relay, while full CSI of the $\boldsymbol{R}\rightarrow\boldsymbol{D}$ channel $\boldsymbol{H}_2$, the $\boldsymbol{R}\rightarrow\boldsymbol{R}$ residual LI channel $\boldsymbol{H}_R$ and the j^{th} interferer channel $\boldsymbol{g}_i$ with $i=1,\,\ldots,\,M_D$ are assumed to be available at the relay and destination. 4) In order to completely eliminate the CCI channel at the relay and destination, the number of relay receive antennas is assumed to be greater than the number of interferers at the relay (i.e., $N_R>M_R$), similarly, the number of antennas at the destination is assumed to be greater than the number of interferers at the destination (i.e., $N_D>M_D$). Likewise, in order to entirely suppress the LI channel at the relay, the number of relay transmit antennas is supposed to be larger than one (i.e., $N_T>1$). These are essential conditions for ensuring the feasibility of the proposed hop-by-hop ZF scheme.

III. The Instantaneous Overall SINR

At time instant n, the received signal at the relay after receive combining vector can be written as

$$\begin{aligned} z_R\left[n\right] &= \boldsymbol{w}_R^{\dagger}\boldsymbol{y}_R\left[n\right] \\ &= \boldsymbol{w}_R^{\dagger}\Bigg(\boldsymbol{H}_1\boldsymbol{w}_S x_S\left[n\right]+\boldsymbol{H}_R\boldsymbol{w}_T x_R\left[n\right] \\ &\qquad +\sum_{i=1}^{M_R}\boldsymbol{h}_i x_i\left[n\right]+\boldsymbol{n}_R\left[n\right]\Bigg), \end{aligned} \tag{1}$$

where $x_S\left[n\right]$ is the transmitted signal with average power $\mathcal{E}_S=\mathbb{E}\left[x_S\left[n\right]x_S^{\star}\left[n\right]\right]$, and $\mathbb{E}\left(\cdot\right)$ denotes the expectation operator, $\left(\cdot\right)^{\star}$ denotes the conjugate operator, $x_R\left[n\right]$ is the relay signal with average power $\mathcal{E}_R=\mathbb{E}\left[x_R\left[n\right]x_R^{\star}\left[n\right]\right]$, $x_i\left[n\right]$ is the i^{th} interference signal at the FD node with average power $\mathcal{E}_i^R=\mathbb{E}\left[x_i\left[n\right]x_i^{\star}\left[n\right]\right]$, $\boldsymbol{n}_R\left[n\right]$ is an $N_R\times 1$ vector which denotes the additive white Gaussian noise (AWGN) at the relay, distributed according to $\boldsymbol{n}_R\left[n\right]\sim\mathcal{CN}\left(0,\,\sigma^2\boldsymbol{I}_{N_R}\right)$,

$\boldsymbol{w}_R$ is the receive combining weight vector at the relay with unit norm, $(\cdot)^\dagger$ denotes the conjugate transpose operator, $\boldsymbol{w}_S$ is the transmit beamforming weight vector at the source with unit norm, and $\boldsymbol{w}_T$ is the transmit beamforming weight vector at the relay with unit norm. Let $\boldsymbol{H} = [\boldsymbol{h}_1, \boldsymbol{h}_2, \ldots, \boldsymbol{h}_{M_R}]$ be the CCI matrix at the relay with dimension $N_R \times M_R$. Then, the term $\sum_{i=1}^{M_R} \boldsymbol{w}_R^\dagger \boldsymbol{h}_i x_i[n]$ in (1) can be re-written as $\boldsymbol{w}_R^\dagger \boldsymbol{H} \boldsymbol{x}_I[n]$ where $\boldsymbol{x}_I[n] = [x_1[n], x_2[n], \ldots, x_{M_R}[n]]^T$, where $(\cdot)^T$ denotes the transpose operator.

The relay transmit signal is given as

$$x_R[n] = \mathcal{G} z_R[n-\tau], \tag{2}$$

where τ is the processing delay time needed at the relay for the FD operation, and $\mathcal{G}$ is the channel assisted (variable gain) relay normalizing constant, and is given by as in (3), as shown at the top of next page.

Due to the recursive nature of (1) and (2), the signal transmitted by the relay is re-written as as in (4), as shown at the top of next page.

The combined received signal at the destination can be written as

$$\begin{aligned} z_D[n] &= \boldsymbol{w}_D^\dagger \boldsymbol{y}_D[n] \\ &= \boldsymbol{w}_D^\dagger \left(\boldsymbol{H}_2 \boldsymbol{w}_T x_R[n] + \sum_{i=1}^{M_D} \boldsymbol{g}_i y_i[n] + \boldsymbol{n}_D[n] \right), \end{aligned} \tag{5}$$

where $\boldsymbol{w}_D$ is the receive combining weight vector at the destination with unit norm, $y_i[n]$ is the i^{th} interferer signal at the destination with average power $\mathcal{E}_i^D = \mathbb{E}[y_i[n] y_i^\star[n]]$ and $\boldsymbol{n}_D[n]$ is the AWGN at the destination and distributed according to $\boldsymbol{n}_D[n] \sim \mathcal{CN}(0, \sigma^2 \boldsymbol{I}_{N_D})$. Let $\boldsymbol{G} = [\boldsymbol{g}_1, \boldsymbol{g}_2, \ldots, \boldsymbol{g}_{M_D}]$ be the CCI matrix at the destination with dimension $N_D \times M_D$. Then, the term $\sum_{i=1}^{M_D} \boldsymbol{w}_D^\dagger \boldsymbol{g}_i y_i[n]$ in (5) can be re-written as $\boldsymbol{w}_D^\dagger \boldsymbol{G} \boldsymbol{y}_I[n]$ where $\boldsymbol{y}_I[n] = [y_1[n], y_2[n], \ldots, y_{M_D}[n]]^T$.

Therefore, the overall SINR may be expressed as[4]

$$\gamma = \frac{\gamma_1 \gamma_2}{\gamma_1 + \gamma_2 + 1}, \tag{6}$$

where

$$\gamma_1 = \frac{\overline{\gamma_1} \left| \boldsymbol{w}_R^\dagger \boldsymbol{H}_1 \boldsymbol{w}_S \right|^2}{\overline{\gamma_2} \left| \boldsymbol{w}_R^\dagger \boldsymbol{H}_R \boldsymbol{w}_T \right|^2 + \left\| \boldsymbol{P}_{I_R}^{\frac{1}{2}} \boldsymbol{H}^\dagger \boldsymbol{w}_R \right\|^2 + 1}, \tag{7}$$

and

$$\gamma_2 = \frac{\overline{\gamma_2} \left| \boldsymbol{w}_D^\dagger \boldsymbol{H}_2 \boldsymbol{w}_T \right|^2}{\left\| \boldsymbol{P}_{I_D}^{\frac{1}{2}} \boldsymbol{G}^\dagger \boldsymbol{w}_D \right\|^2 + 1}, \tag{8}$$

where $\overline{\gamma_1} = \frac{\mathcal{E}_S}{\sigma^2}$, $\overline{\gamma_2} = \frac{\mathcal{E}_R}{\sigma^2}$, while the interference-to-noise ratio at the relay is expressed as $\sum_{i=1}^{M_R} \left| \boldsymbol{w}_R^\dagger \boldsymbol{h}_i \right|^2 \frac{\mathcal{E}_i^R}{\sigma^2} = \left\| P_{I_R}^{\frac{1}{2}} \boldsymbol{H}^\dagger \boldsymbol{w}_R \right\|^2$, with $\|\cdot\|$ denotes the Euclidean norm operator, and $\boldsymbol{P}_{I_R}$ is a diagonal matrix given as $\boldsymbol{P}_{I_R} = \operatorname{diag}\left(\rho_1^R, \rho_2^R, \ldots, \rho_{M_R}^R\right)$, $\rho_i^R = \frac{\mathcal{E}_i^R}{\sigma^2}$. Similarly, the interference-to-noise ratio at the destination may be written as $\sum_{i=1}^{M_D} \left| \boldsymbol{w}_D^\dagger \boldsymbol{g}_i \right|^2 \frac{\mathcal{E}_i^D}{\sigma^2} = \left\| P_{I_D}^{\frac{1}{2}} \boldsymbol{G}^\dagger \boldsymbol{w}_D \right\|^2$, where $\boldsymbol{P}_{I_D}$ is a diagonal matrix defined as $\boldsymbol{P}_{I_D} = \operatorname{diag}\left(\rho_1^D, \rho_2^D, \ldots, \rho_{M_D}^D\right)$, and $\rho_i^D = \frac{\mathcal{E}_i^D}{\sigma^2}$.

Proof: Please see Appendix A for the proof. ∎

The main goal is to attain an optimal source beamforming vector, destination combining vector, and relay beamforming and combining vectors, i.e., finding $\boldsymbol{w} = \{\boldsymbol{w}_S, \boldsymbol{w}_R, \boldsymbol{w}_T, \boldsymbol{w}_D\}$ so as to maximize the overall SINR in (6). Therefore, the optimization problem may be formulated as follows

$$\begin{aligned} \boldsymbol{w}^\star = \arg\max_{\boldsymbol{w}} \; & \gamma \,(\text{in Eq. (6)}) \\ \text{s. t. } & \|\boldsymbol{w}\| = 1, \end{aligned} \tag{9}$$

where $\boldsymbol{w}^\star = \{\boldsymbol{w}_S^\star, \boldsymbol{w}_R^\star, \boldsymbol{w}_T^\star, \boldsymbol{w}_D^\star\}$. It is widely common that in the absence of interference, MRT and MRC at the transmitter and the receiver, respectively, are optimal beamforming and combining schemes as they yield the maximum overall SINR [29]–[31]. However, owing to the deleterious frequency reuse in FD relaying networks, where more detrimental effects of CCI will be experienced as the amount of CCI is predicted to double in contrast to its traditional HD relaying counterpart [1], MRC and MRT become sub-optimal as they treat the interference as additive noise. Therefore, the existence of CCI can seriously deteriorate the performance of FD relaying networks, and hence its mitigation is of practical importance. Due to the complexity of the optimization formula in (9), the optimal receive (transmit) decoding (precoding) weight vectors at the source, MIMO FD relay, and the destination are nontrivial to obtain in closed-form. Therefore, to derive a closed-form mathematically tractable overall SINR, a sub-optimal formula is proposed by inserting a receive and transmit null space projection constraints to the optimization problem in (9). These constraints force the loopback self and co-channel interference terms at the relay and destination to zero, i.e., $\boldsymbol{w}_R^\dagger \boldsymbol{H}_R \boldsymbol{w}_T = 0$, $\boldsymbol{H}^\dagger \boldsymbol{w}_R = 0$, and $\boldsymbol{G}^\dagger \boldsymbol{w}_D = 0$, assuming that $N_R > M_R$, $N_T > 1$, and $N_D > M_D$. To this end, because of the separability of the attained constraint problem, this problem may be decoupled into two manageable problems as follows

$$\begin{aligned} \boldsymbol{w}^\star = \arg\max_{\boldsymbol{w}_S, \boldsymbol{w}_R} \; & \left\| \boldsymbol{w}_R^\dagger \boldsymbol{H}_1 \boldsymbol{w}_S \right\|^2 \\ \text{s. t. } & \boldsymbol{H}^\dagger \boldsymbol{w}_R = 0 \;\&\; \|\boldsymbol{w}\| = 1, \end{aligned} \tag{10}$$

and

$$\begin{aligned} \boldsymbol{w}^\star = \arg\max_{\boldsymbol{w}_T, \boldsymbol{w}_D} \; & \left\| \boldsymbol{w}_D^\dagger \boldsymbol{H}_2 \boldsymbol{w}_T \right\|^2 \\ \text{s. t. } & \boldsymbol{G}^\dagger \boldsymbol{w}_D = 0 \;\&\; \boldsymbol{w}_R^\dagger \boldsymbol{H}_R \boldsymbol{w}_T = 0 \;\&\; \|\boldsymbol{w}\| = 1. \end{aligned} \tag{11}$$

Proposition 1: The optimal solution to the constraint optimization problems in (10) and (11) are (respectively) derived as

$$\boldsymbol{w}_R^\star = \frac{\boldsymbol{P}_{\boldsymbol{H}_1} \boldsymbol{u}_{\max}\left(\boldsymbol{H}_1^\dagger \boldsymbol{P}_{\boldsymbol{H}_1} \right)}{\left\| \boldsymbol{P}_{\boldsymbol{H}_1} \boldsymbol{u}_{\max}\left(\boldsymbol{H}_1^\dagger \boldsymbol{P}_{\boldsymbol{H}_1} \right) \right\|}, \tag{12}$$

[4]Note that the $\boldsymbol{S} \to \boldsymbol{R}$ SINR (γ_1) and the $\boldsymbol{R} \to \boldsymbol{D}$ SINR (γ_2) in (7) and (8) could alternatively be derived straightforwardly from (1) and (5), respectively. This formulation has been extensively used in the full duplex relaying literature, see e.g., [10, eq. (6)], [26, eq. (5)], and [28, eq. (11)].

$$\mathcal{G} = \sqrt{\frac{\mathcal{E}_R}{\mathbb{E}\left(\left|z_R\left[n\right]\right|^2\right)}} = \sqrt{\frac{\mathcal{E}_R}{\mathcal{E}_S\left|\boldsymbol{w}_R^\dagger \boldsymbol{H}_1 \boldsymbol{w}_S\right|^2 + \mathcal{E}_R\left|\boldsymbol{w}_R^\dagger \boldsymbol{H}_R \boldsymbol{w}_T\right|^2 + \sum_{i=1}^{M_R}\left|\boldsymbol{w}_R^\dagger \boldsymbol{h}_i\right|^2 \mathcal{E}_i^R + \sigma^2}}. \tag{3}$$

$$\begin{aligned} x_R\left[n\right] &= \mathcal{G}\boldsymbol{w}_R^\dagger\left(\boldsymbol{H}_1\boldsymbol{w}_S x_S\left[n-\tau\right] + \boldsymbol{H}_R\boldsymbol{w}_T\mathcal{G}z_R\left[n-2\tau\right] + \sum_{i=1}^{M_R}\boldsymbol{h}_i x_i\left[n-\tau\right] + \boldsymbol{n}_R\left[n-\tau\right]\right) \\ &= \sum_{j=0}^{\infty}\left(\boldsymbol{w}_R^\dagger\boldsymbol{H}_R\boldsymbol{w}_T\mathcal{G}\right)^j \mathcal{G}\boldsymbol{w}_R^\dagger\left(\boldsymbol{H}_1\boldsymbol{w}_S x_S\left[n-j\tau-\tau\right] + \sum_{i=1}^{M_R}\boldsymbol{h}_i x_i\left[n-j\tau-\tau\right] + \boldsymbol{n}_R\left[n-j\tau-\tau\right]\right). \end{aligned} \tag{4}$$

and

$$\boldsymbol{w}_S^\star = \boldsymbol{u}_{\max}\left(\boldsymbol{H}_1^\dagger\boldsymbol{P}\boldsymbol{H}_1\right), \tag{13}$$

and

$$\boldsymbol{w}_D^\star = \frac{\boldsymbol{B}\boldsymbol{H}_2\boldsymbol{D}\boldsymbol{u}_{\max}\left(\boldsymbol{D}\boldsymbol{H}_2^\dagger\boldsymbol{B}\boldsymbol{H}_2\boldsymbol{D}\right)}{\left\|\boldsymbol{B}\boldsymbol{H}_2\boldsymbol{D}\boldsymbol{u}_{\max}\left(\boldsymbol{D}\boldsymbol{H}_2^\dagger\boldsymbol{B}\boldsymbol{H}_2\boldsymbol{D}\right)\right\|}, \tag{14}$$

and

$$\boldsymbol{w}_T^\star = \frac{\boldsymbol{D}\boldsymbol{u}_{\max}\left(\boldsymbol{D}\boldsymbol{H}_2^\dagger\boldsymbol{B}\boldsymbol{H}_2\boldsymbol{D}\right)}{\left\|\boldsymbol{D}\boldsymbol{u}_{\max}\left(\boldsymbol{D}\boldsymbol{H}_2^\dagger\boldsymbol{B}\boldsymbol{H}_2\boldsymbol{D}\right)\right\|}, \tag{15}$$

where $\boldsymbol{u}_{\max}\left(\boldsymbol{X}^\dagger\boldsymbol{X}\right)$, $\boldsymbol{X} \in \{\boldsymbol{P}\boldsymbol{H}_1, \boldsymbol{B}\boldsymbol{H}_2\boldsymbol{D}\}$ *is the right or left singular vector of the channel matrix* $\boldsymbol{X}^\dagger\boldsymbol{X}$ *corresponding to the strongest eigenmode, i.e., the eigenvector corresponding to* $\lambda_{\max}\left(\boldsymbol{X}^\dagger\boldsymbol{X}\right)$*, the largest eigenvalue of the Wishart matrix* $\boldsymbol{X}^\dagger\boldsymbol{X}$*. Note that* $\lambda_{\max}\left(\boldsymbol{X}^\dagger\boldsymbol{X}\right) = \|\boldsymbol{X}\|_2^2$*. The null space projection matrices* $\boldsymbol{P}$*,* $\boldsymbol{B}$*, and* $\boldsymbol{D}$ *are (respectively) given as* $\boldsymbol{P} = \boldsymbol{I}_{N_R} - \boldsymbol{H}\left(\boldsymbol{H}^\dagger\boldsymbol{H}\right)^{-1}\boldsymbol{H}^\dagger$*,* $\boldsymbol{B} = \boldsymbol{I}_{N_D} - \boldsymbol{G}\left(\boldsymbol{G}^\dagger\boldsymbol{G}\right)^{-1}\boldsymbol{G}^\dagger$*, and* $\boldsymbol{D} = \boldsymbol{I}_{N_T} - \frac{\boldsymbol{H}_R^\dagger\boldsymbol{P}\boldsymbol{H}_1\boldsymbol{w}_S^\star\left(\boldsymbol{H}_R^\dagger\boldsymbol{P}\boldsymbol{H}_1\boldsymbol{w}_S^\star\right)^\dagger}{\left(\boldsymbol{H}_R^\dagger\boldsymbol{P}\boldsymbol{H}_1\boldsymbol{w}_S^\star\right)^\dagger\boldsymbol{H}_R^\dagger\boldsymbol{P}\boldsymbol{H}_1\boldsymbol{w}_S^\star}$.

Proof: Please see Appendix B for the proof. ∎

Note that in the proposed ZF beamforming scheme, the optimal source and relay transmit powers are given by their maximum values, i.e., $\mathcal{E}_S$ and $\mathcal{E}_R$, respectively, as they result in the maximum overall SINR. This is due to the absence of the direct link channel between the source and the destination, while the impact of the relay transmit signal on its received signal is removed through null space projections, via the added ZF constraint, $\boldsymbol{w}_R^\dagger\boldsymbol{H}_R\boldsymbol{w}_T = 0$.

Therefore, the overall SINR of MIMO FD relaying with LI and CCI by utilizing hop-by-hop ZF beamforming can be derived as [32]

$$\gamma = \frac{\gamma_1\gamma_2}{\gamma_1 + \gamma_2 + 1}, \tag{16}$$

where $\gamma_1 = \overline{\gamma_1}\lambda_{\max}\left(\boldsymbol{H}_1^\dagger\boldsymbol{P}\boldsymbol{H}_1\right) = \overline{\gamma_1}\|\boldsymbol{P}\boldsymbol{H}_1\|_2^2$, $\gamma_2 = \overline{\gamma_2}\lambda_{\max}\left(\boldsymbol{D}\boldsymbol{H}_2^\dagger\boldsymbol{B}\boldsymbol{H}_2\boldsymbol{D}\right) = \overline{\gamma_2}\|\boldsymbol{B}\boldsymbol{H}_2\boldsymbol{D}\|_2^2$.

Note that the matrices $\boldsymbol{P}$, $\boldsymbol{B}$ and $\boldsymbol{D}$ are idempotent orthogonal projection (null-space projection) matrices (i.e., all their eigenvalues are either one or zero, where the number of ones is determined by the rank of the matrix)[5] which are used to eliminate the co-channel interference at the relay, destination and loopback self-interference channel at the relay, respectively. For instance, in the case of idempotent orthogonal projection matrix $\boldsymbol{P}$, we have $\mathrm{tr}\left(\boldsymbol{P}\right) = \mathrm{rank}\left(\boldsymbol{P}\right)$ because of idempotency, where $\mathrm{tr}\left(\cdot\right)$ denotes the trace operation. Hence, we have

$$\begin{aligned} \mathrm{rank}\left(\boldsymbol{P}\right) &= \mathrm{rank}\left(\boldsymbol{I}_{N_R} - \boldsymbol{G}\left(\boldsymbol{G}^\dagger\boldsymbol{G}\right)^{-1}\boldsymbol{G}^\dagger\right) \\ &= \mathrm{rank}\left(\boldsymbol{I}_{N_R}\right) - \mathrm{rank}\left(\boldsymbol{G}\left(\boldsymbol{G}^\dagger\boldsymbol{G}\right)^{-1}\boldsymbol{G}^\dagger\right). \end{aligned} \tag{17}$$

It can be easily shown that $\mathrm{rank}\left(\boldsymbol{I}_{N_R}\right) = N_R$ and $\mathrm{rank}\left(\boldsymbol{G}\left(\boldsymbol{G}^\dagger\boldsymbol{G}\right)^{-1}\boldsymbol{G}^\dagger\right) = \mathrm{rank}\left(\boldsymbol{G}\right) = M_R$. Hence, $\mathrm{rank}\left(\boldsymbol{P}\right) = N_R - M_R$. Similarly, it can be shown that $\mathrm{rank}\left(\boldsymbol{B}\right) = N_D - M_D$, and $\mathrm{rank}\left(\boldsymbol{D}\right) = N_T - 1$.

Therefore, it is easily shown that $\|\boldsymbol{P}\boldsymbol{H}_1\|_2^2$ and $\|\boldsymbol{B}\boldsymbol{H}_2\boldsymbol{D}\|_2^2$ are the largest eigenvalue of the Wishart matrices $\boldsymbol{P}\boldsymbol{H}_1$ and $\boldsymbol{B}\boldsymbol{H}_2\boldsymbol{D}$ with dimensions $(N_R - M_R) \times N_S$ and $(N_D - M_D) \times (N_T - 1)$, respectively [8], [15]. Hence, the cumulative distribution function (CDF) and probability density function (PDF) of γ_1 and γ_2, respectively, are given as [30]

$$F_{\gamma_1}\left(x\right) = 1 - \sum_{i=1}^{s_1}\sum_{j=t_1-s_1}^{(t_1+s_1-2i)i}\sum_{k=0}^{j}\frac{i^k d_1\left(i,\,j\right)}{k!\overline{\gamma_1}^k}x^k e^{-\frac{ix}{\overline{\gamma_1}}}, \tag{18}$$

and

$$f_{\gamma_2}\left(y\right) = \sum_{l=1}^{s_2}\sum_{m=t_2-s_2}^{(t_2+s_2-2l)l}\frac{l^{m+1}d_2\left(l,\,m\right)}{m!\overline{\gamma_2}^{m+1}}y^m e^{-\frac{ly}{\overline{\gamma_2}}}, \tag{19}$$

where $s_1 = \min\left(N_S,\, N_R - M_R\right)$, $t_1 = \max(N_S,\, N_R - M_R)$, $s_2 = \min(N_T - 1,\, N_D - M_D)$, $t_2 = \max(N_T - 1,\, N_D - M_D)$, and the coefficients $d_c\left(a,\,b\right)$, $c = 1, 2$ are given in [30] for some system configurations, and they can be efficiently evaluated for any arbitrary configurations by using [31, Algorithm 1].

A. MRT/MRC Scheme

In dual-hop relaying systems, hop-by-hop MRT beamforming is utilized to steer the transmitted signal along the strongest eigenmode of each hop's channel (see e.g., [34], [35]).

[5]It is well known that the rank of an $M \times N$ matrix A is $\mathrm{rank}\left(A\right) \leq \min\left(M,\,N\right)$, where equality holds if and only if A is full rank [33].

Hence, in the presence of perfect CSI of $\boldsymbol{H}_1$ and $\boldsymbol{H}_2$, and in the absence of full CSI of $\boldsymbol{H}_R$, $\boldsymbol{H}$, and $\boldsymbol{G}$, the first hop MRT beamformers $\boldsymbol{w}_S$ and $\boldsymbol{w}_R$ are set to match $\boldsymbol{v}_{\max}\left(\boldsymbol{H}_1^{\dagger}\boldsymbol{H}_1\right)$ and $\boldsymbol{u}_{\max}\left(\boldsymbol{H}_1\boldsymbol{H}_1^{\dagger}\right)$, the left or right singular vector of the channel matrix $\boldsymbol{H}_1^{\dagger}\boldsymbol{H}_1$ and $\boldsymbol{H}_1\boldsymbol{H}_1^{\dagger}$ (respectively) corresponding to the strongest eigenmode of the Wishart matrix $\boldsymbol{H}_1^{\dagger}\boldsymbol{H}_1$ [35, eq. (7)]. Similarly, the second hop MRT beamformers $\boldsymbol{w}_T$ and $\boldsymbol{w}_D$ are set to match $\boldsymbol{v}_{\max}\left(\boldsymbol{H}_2^{\dagger}\boldsymbol{H}_2\right)$ and $\boldsymbol{u}_{\max}\left(\boldsymbol{H}_2\boldsymbol{H}_2^{\dagger}\right)$, the left or right singular vector of the channel matrix $\boldsymbol{H}_2^{\dagger}\boldsymbol{H}_2$ and $\boldsymbol{H}_2\boldsymbol{H}_2^{\dagger}$ (respectively) corresponding to the strongest eigenmode of the Wishart matrix $\boldsymbol{H}_2^{\dagger}\boldsymbol{H}_2$. Note that MRT beamforming requires full CSI for $\boldsymbol{H}_1$, $\boldsymbol{H}_2$ only, while ZF beamforming requires full CSI for $\boldsymbol{H}_1$, $\boldsymbol{H}_2$, $\boldsymbol{H}_R$, $\boldsymbol{H}$, and $\boldsymbol{G}$. Meanwhile, in the absence of $\boldsymbol{H}_R$, $\boldsymbol{H}$, and $\boldsymbol{G}$, ZF beamforming reduces to MRT beamforming.

Therefore, from (6)-(8), the overall SINR for MRT beamforming reduces to

$$\gamma^{\text{MRT}} = \frac{\gamma_1^{\text{MRT}}\gamma_2^{\text{MRT}}}{\gamma_1^{\text{MRT}} + \gamma_2^{\text{MRT}} + 1}, \tag{20}$$

where γ_1^{MRT} is given as in (21), as shown at the top of next page, and

$$\gamma_2^{\text{MRT}} = \frac{\overline{\gamma_2}\left\|\boldsymbol{H}_2\right\|_2^2}{\left\|P_{I_D}^{\frac{1}{2}}\boldsymbol{G}^{\dagger}\boldsymbol{u}_{\max}\left(\boldsymbol{H}_2\boldsymbol{H}_2^{\dagger}\right)\right\|^2 + 1}, \tag{22}$$

where $\left\|\boldsymbol{H}_i\right\|_2^2 = \lambda_{\max}\left(\boldsymbol{H}_i^{\dagger}\boldsymbol{H}_i\right)$, the largest eigenvalue of the Wishart matrix $\boldsymbol{H}_i^{\dagger}\boldsymbol{H}_i$, $i \in \{1,\, 2\}$.

Due to the analytical complexity of evaluating the performance of (20), only simulation results are included in this paper for comparison purposes.

IV. Outage Probability Analysis

In this section, the information outage probability of MIMO FD relaying systems with hop-by-hop ZF beamfoming is investigated. An exact expression for the outage probability is derived in closed-form. The outage probability is defined as the probability that the instantaneous mutual information, $\mathcal{I} = \log_2(1+\gamma)$, drops under a target rate of R_0 bits per channel use[6]

$$\begin{aligned} \mathrm{P}_{\text{out}}(R_0) &= \Pr\left(\log_2(1+\gamma) < R_0\right) \\ &= F_{\gamma}(\gamma_T). \end{aligned} \tag{23}$$

where $\gamma_T = 2^{R_0} - 1$, and $F_{\gamma}(\cdot)$ denotes the CDF of the overall SINR.

[6]Note that in contrast to (23), the SINR outage probability can be defined as the probability that the instantaneous overall γ falls below a threshold γ_T; $\Pr(\gamma < \gamma_T) = F_{\gamma}(\gamma_T)$. Note that according to (23), γ_T in the case of half-duplex relaying is given as $\gamma_T = 2^{2R_0} - 1$.

A. Accurate Outage Probability

The CDF of the overall SINR can be defined as [34, Appendix I]

$$\begin{aligned} F_{\gamma}(\gamma_T) &= \Pr\left(\frac{\gamma_1\gamma_2}{\gamma_1+\gamma_2+1} < \gamma_T\right) \\ &= 1 - \int_0^{\infty} \overline{F}_{\gamma_1}\left(\frac{\gamma_T(\gamma_T+w+1)}{w}\right) f_{\gamma_2}(\gamma_T+w)\, dw, \end{aligned} \tag{24}$$

where $\overline{F}_{\gamma_1}(\cdot)$ is the complementary CDF of γ_1.

Proposition 2: An exact closed-form outage probability expression for MIMO FD relaying systems with loopback self-interference, M_R and M_D co-channel interferers at the relay and destination, with hop-by-hop ZF beamfoming, can be expressed as in (25), as shown at the top of next page, where $\mathcal{K}_v(z)$ is the modified bessel function of the second kind of order v.

Proof: Please see Appendix C for the proof. ■

B. Outage Probability Lower-Bound

Even though proposition 2 yields an effective ways for evaluating accurate outage probability, this expression is fairly involved since no simple insights into the performance of the system can be attained. The overall SINR in (16) could be easily upper-bounded by[7]

$$\gamma \le \gamma_{\text{up}} = \min(\gamma_1,\, \gamma_2). \tag{26}$$

Hence, the outage probability lower-bound formula for multi-antenna FD relaying networks with hop-by-hop ZF beamfoming can be expressed as

$$\begin{aligned} F_{\gamma_{\text{up}}}(\gamma_T) = 1 - &\sum_{i=1}^{s_1} \sum_{j=t_1-s_1}^{(t_1+s_1-2i)i} d_1(i,\, j)\, \frac{\Gamma\left(j+1,\, \frac{i\gamma_T}{\overline{\gamma_1}}\right)}{j!} \\ &\times \sum_{l=1}^{s_2} \sum_{m=t_2-s_2}^{(t_2+s_2-2l)l} d_2(l,\, m)\, \frac{\Gamma\left(m+1,\, \frac{l\gamma_T}{\overline{\gamma_2}}\right)}{m!}. \end{aligned} \tag{27}$$

Proof: Please see Appendix D for the proof. ■

In the following, the outage probability lower-bound formula in (27) is utilized to attain an asymptotic approximations for the outage probability of multi-antenna FD relaying networks with hop-by-hop ZF beamfoming.

1) Asymptotic Approximations: To certify and specify the attainable diversity order of the multi-antenna FD relaying networks with with LI, M_R and M_D co-channel interferers at the relay and destination, employing hop-by-hop ZF beamfoming, (27) is employed in the asymptotically high SNR reign by letting $\overline{\gamma_2} = \kappa\overline{\gamma_1}$, where κ denotes a finite fixed integer

[7]To simplify the analytical complexity and attain preferable insights into the system performance, we utilize the well-known fact in the conventional half-duplex relaying literature that the overall SNR $\gamma = \frac{\gamma_1\gamma_2}{\gamma_1+\gamma_2+1}$ could be firmly upper-bounded as $\frac{\gamma_1\gamma_2}{\gamma_1+\gamma_2}$ (see e.g., [36, eq. (6)]). Note that the upper-bound $\frac{\gamma_1\gamma_2}{\gamma_1+\gamma_2}$ may further be upper-bounded by $\min(\gamma_1,\, \gamma_2)$ (see e.g., [19, eq. (8)]).

$$\gamma_1^{\text{MRT}} = \frac{\overline{\gamma_1}\left\|\boldsymbol{H}_1\right\|_2^2}{\overline{\gamma_2}\left|\boldsymbol{u}_{\max}^{\dagger}\left(\boldsymbol{H}_1\boldsymbol{H}_1^{\dagger}\right)\boldsymbol{H}_R\boldsymbol{v}_{\max}\left(\boldsymbol{H}_2^{\dagger}\boldsymbol{H}_2\right)\right|^2 + \left\|P_{I_R}^{\frac{1}{2}}\boldsymbol{H}^{\dagger}\boldsymbol{u}_{\max}\left(\boldsymbol{H}_1\boldsymbol{H}_1^{\dagger}\right)\right\|^2 + 1}, \tag{21}$$

$$F_{\gamma}\left(\gamma_T\right) = 1 - 2\sum_{i=1}^{s_1}\sum_{j=t_1-s_1}^{(t_1+s_1-2i)i}\sum_{k=0}^{j}\frac{i^k d_1\left(i,\,j\right)}{k!\overline{\gamma_1}^k}\gamma_T^k e^{-i\frac{\gamma_T}{\overline{\gamma_1}}}\sum_{p=0}^{k}\binom{k}{p}\left(\gamma_T+1\right)^p\sum_{l=1}^{s_2}\sum_{m=t_2-s_2}^{(t_2+s_2-2l)l}\frac{l^{m+1}d_2\left(l,\,m\right)}{m!\overline{\gamma_2}^{m+1}}$$
$$\times\, e^{-\frac{l\gamma_T}{\overline{\gamma_2}}}\sum_{n=0}^{m}\binom{m}{n}\gamma_T^{m-n}\left(\frac{i\gamma_T\overline{\gamma_2}\left(\gamma_T+1\right)}{l\overline{\gamma_1}}\right)^{\frac{n-p+1}{2}}\mathcal{K}_{n-p+1}\left(2\sqrt{\frac{il\gamma_T\left(\gamma_T+1\right)}{\overline{\gamma_1}\overline{\gamma_2}}}\right), \tag{25}$$

$$F_{\gamma}^{\infty}\left(\gamma_T\right) = \frac{\prod_{l=0}^{s_1-1}l!}{\prod_{l=0}^{s_1-1}\left(t_1+l\right)!}\left(\frac{\gamma_T}{\overline{\gamma_1}}\right)^{N_S\left(N_R-M_R\right)} + \frac{\prod_{l=0}^{s_2-1}l!}{\prod_{l=0}^{s_2-1}\left(t_2+l\right)!}\left(\frac{\gamma_T}{\overline{\gamma_2}}\right)^{\left(N_T-1\right)\left(N_D-M_D\right)}$$
$$+ O\left(\left(\frac{\gamma_T}{\overline{\gamma_1}}\right)^{\min\left(N_S\left(N_R-M_R\right),\,\left(N_T-1\right)\left(N_D-M_D\right)\right)+1}\right). \tag{28}$$

and $\overline{\gamma_1} \to \infty$. Therefore, the asymptotic approximations for the outage probability can be expressed as in (28), as shown at the top of this page.

Proof: Please see Appendix E for the proof. ■

It is straight forward to show from (28) that the achievable diversity order of the MIMO FD relaying system with LI, M_R and M_D co-channel interferers at the relay and destination, utilizing hop-by-hop ZF beamfoming scheme is $\min\left(N_S\left(N_R-M_R\right),\,\left(N_T-1\right)\left(N_D-M_D\right)\right)$.

V. Ergodic Capacity Analysis

In this section, we present a rigorous investigation on the ergodic capacity of MIMO FD relaying systems with LI, M_R and M_D co-channel interferers at the relay and destination, utilizing hop-by-hop ZF beamfoming. The ergodic capacity is defined as the expected value of the instantaneous mutual information between the source and destination, and is given by

$$C = \frac{1}{\ln 2}\mathbb{E}\left[\ln\left(1+\gamma\right)\right] = \frac{1}{\ln 2}\mathbb{E}\left[\ln\left(1+\frac{\gamma_1\gamma_2}{\gamma_1+\gamma_2+1}\right)\right]. \tag{29}$$

A. Accurate Ergodic Capacity

To lower the analytical evaluation difficulties, the following lemma is utilized to modify (29) into a better and suitable form that enables the evaluation of the needed average via familiar formulas of moment generating functions (MGFs).

Lemma 1: For any two random variables $X \geq 0$ and $Y \geq 0$, where X and Y are independent, we have [26, Lemma 3]

$$\mathbb{E}\left[\ln\left(1+\frac{XY}{X+Y+1}\right)\right] = \int_0^{\infty}\frac{1}{z}\left(1-\mathcal{M}_X\left(z\right)\right)\left(1-\mathcal{M}_Y\left(z\right)\right)e^{-z}dz, \tag{30}$$

where $\mathcal{M}_X\left(z\right) = \mathbb{E}\left(e^{-zX}\right)$ is the MGF of X, and $\mathcal{M}_Y\left(z\right) = \mathbb{E}\left(e^{-zY}\right)$ is the MGF of Y.

Let $X = \gamma_1 = \overline{\gamma_1}\left\|\boldsymbol{P}\boldsymbol{H}_1\right\|_2^2$, $Y = \gamma_2 = \overline{\gamma_2}\left\|\boldsymbol{B}\boldsymbol{H}_2\boldsymbol{D}\right\|_2^2$. Therefore, the MGFs of γ_k is given as [34, eq. (20)]

$$\mathcal{M}_{\gamma_k}\left(z\right) = \sum_{i=1}^{s_k}\sum_{j=t_k-s_k}^{(t_k+s_k-2i)i}\frac{d_k\left(i,\,j\right)}{\left(\frac{\overline{\gamma_k}}{i}z+1\right)^{j+1}}, \tag{31}$$

where $k \in \{1,\,2\}$.

Proposition 3: An exact closed-form ergodic capacity expression for MIMO FD relaying systems with LI, M_R and M_D co-channel interferers at the relay and destination, utilizing hop-by-hop ZF beamfoming, can be derived as in (32), as shown at the bottom of next page, where $G^{\cdot,\cdot}_{\cdot,\cdot}\left(.\,|.\right)$ is the Meijer's G-function [37, eq. (9.301)], $G^{1,\,1,\,1,\,1}_{1,[1:1],\,0,\,[1:1]}\left(.\,|.\right)$ is the extended generalized bivariate Meijer's G-function [38].

Proof: Please see Appendix F for the proof. ■

B. Ergodic Capacity Lower-Bound

To get a simple lower-bound formula for the ergodic capacity (29), let us re-write (29) in an easier alternative form as follows

$$C = \mathbb{E}\left[\log_2\left(\frac{\left(1+\gamma_1\right)\left(1+\gamma_2\right)}{\gamma_1+\gamma_2+1}\right)\right] = C_{\gamma_1} + C_{\gamma_2} - C_{\gamma_T}, \tag{33}$$

where $C_{\gamma_i} = \mathbb{E}\left[\log_2\left(1+\gamma_i\right)\right]$, for $i \in \{1,\,2\}$, and $C_{\gamma_T} = \mathbb{E}\left[\log_2\left(1+\gamma_1+\gamma_2\right)\right]$. Here, an easier lower-bound formula for C_{γ_T} is presented by utilizing Jensen's inequality to C_{γ_T} as follows

$$C_{\gamma_T} \leq \log_2\left(1+\mathbb{E}\left(\gamma_1\right)+\mathbb{E}\left(\gamma_2\right)\right). \tag{34}$$

Hence, a simple ergodic capacity lower-bound formula for (29) is derived as in (35), as shown at the bottom of next page, where $\mathrm{E}_n\left(\cdot\right)$ denotes the exponential integral function [39, eq. (5.1.4)].

Proof: Please see Appendix G for the proof. ■

VI. Numerical Results

In this section, we validate the presented theoretical results with Monte Carlo simulations. In addition, the impact of

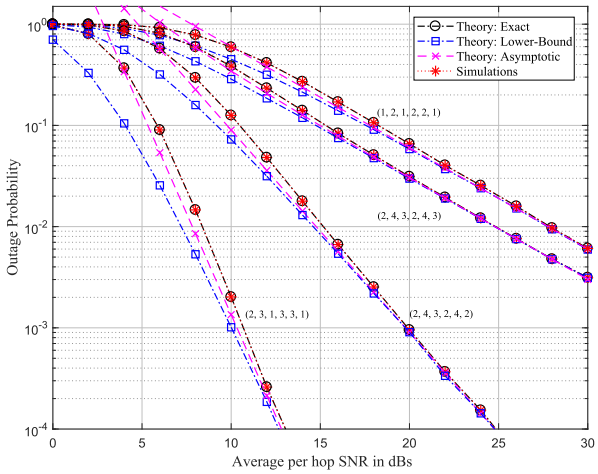

Fig. 2. Multi-antenna FD relaying outage probability against the first-hop SNR ($\overline{\gamma_1}$) where $\overline{\gamma_1} = \overline{\gamma_2}$, with $R_0 = 2$ bits/sec/Hz, and for different settings $(N_S,\, N_R,\, M_R,\, N_T,\, N_D,\, M_D)$.

key system parameters on the outage probability and ergodic capacity performance is investigated. Without loss of generality, a symmetric settings of per-hop SNR is assumed, i.e., $\overline{\gamma_1} = \overline{\gamma_2}$. In addition, the source transmission rate is set to $R_0 = 2$ bits/sec/Hz. Hence, the pre-defined SNR threshold is given as[8] $\gamma_T = 2^{R_0} - 1 = 3$. Besides, specific values for N_S, N_R, M_R, N_T, N_D, and M_D for each antenna configurations are labeled as $(N_S,\, N_R,\, M_R,\, N_T,\, N_D,\, M_D)$ in the figures. For comparison purposes, results for the case of MIMO HD relaying with CCI at the relay and destination and hop-by-hop ZF beamforming are included with the constraint that the total number of antennas at the HD relay is $N = N_R + N_T$. In addition, the number of interferers at the FD relay is chosen to be M_R, which is doubled compared to its HD counterpart. Therefore, each antenna configuration in the case of MIMO HD relaying is denoted in the figures as HD $\left(N_S,\, N_R + N_T,\, \frac{M_R}{2}, N_D,\, M_D\right)$. This refers to the so called number of antenna preserved condition at the relay.

In Fig. 2, the outage probability of MIMO FD relaying against the first-hop SNR is presented, where Monte Carlo simulations of (23) is used to validate the new exact closed-form, lower-bound, and asymptotic mathematical formulas in (25), (27), and (28) respectively. It can be observed that the simulation and proposed exact analytical expression in (25) provide a perfect match which corroborates the accuracy of the proposed closed-form analytical expression. Furthermore, the tightness of the proposed lower-bound and asymptotic analytical expressions in (27) and (28) are also verified, where they become identical at high SNRs. It is clearly seen that increasing the number of antennas and/or the average per-hop SNR significantly improves the outage probability of the system. However, the negative impact of the number of co-channel interferers on the system performance is also verified. The outage probability of multi-antenna FD relaying networks in Fig. 2 outperforms its multi-antenna HD relaying networks counterpart at low SNRs. However, at high SNRs, the outage probability of multi-antenna HD relaying networks is superior. The implementations reveal an exciting insight that is useful in managing the design of multi-antenna FD relaying networks. The attainable diversity orders in Fig. 2, defined as $\min\left(N_S\left(N_R - M_R\right),\, \left(N_T - 1\right)\left(N_D - M_D\right)\right)$, are one, one, two, and four. It is observed that the diversity order is much significant on the outage probability enhancement in contrast to the effect of array gain. For example, the frameworks $(1,\, 2,\, 1,\, 2,\, 2,\, 1)$ and $(2,\, 4,\, 3,\, 2,\, 4,\, 3)$ have similar diversity orders (one). However, the last has a little performance improvement resulting from higher array gain. On the other hand, the settings $(1,\, 2,\, 1,\, 2,\, 2,\, 1)$ and $(2,\, 3,\, 1,\, 3,\, 3,\, 1)$ enjoy diversity orders of one and four, respectively. Thereby, the last benefits from a considerable outage performance enhancement. Notice that when the average SNRs at the source and relay are equal, i.e., $\overline{\gamma_1} = \overline{\gamma_2}$, network settings that have similar diversity order and degrees of freedom have similar performance. For instance, the frameworks $(2,\, 3,\, 2,\, 3,\, 2,\, 1)$ and $(2,\, 5,\, 4,\, 2,\, 4,\, 2)$ enjoy similar outage performance. Hence, for outstanding network performance, the network engineer needs to carefully choose N_S, N_R, N_T, and N_D in order to attain the best feasible diversity order, more specifically, selecting N_S, N_R, N_T, and N_D so that $N_S\left(N_R - M_R\right) \approx \left(N_T - 1\right)\left(N_D - M_D\right)$. It is worth noticing that in the case of fixed infrastructure FD base station relay, N_R and N_T could be higher than that of N_S and N_D due to space constraints at the mobile users.

Fig. 3 shows the ergodic capacity of MIMO FD relaying against the first-hop SNR. simulations results of (29) is exploited to affirm the accurate closed-form and lower-bound mathematical formulas in (32) and (35), respectively. It is seen

[8]Note that for the HD mode, the SNR threshold is written as $\gamma_T = 2^{2R_0} - 1 = 15$.

$$C = \frac{\overline{\gamma_1}\,\overline{\gamma_2}}{\ln 2}\sum_{i=1}^{s_1}\sum_{j=t_1-s_1}^{(t_1+s_1-2i)i}\sum_{k=0}^{j}\frac{d_1\left(i,\, j\right)}{i\Gamma\left(k+1\right)}\sum_{l=1}^{s_2}\sum_{m=t_2-s_2}^{(t_2+s_2-2l)l}\sum_{n=0}^{m}\frac{d_2\left(l,\, m\right)}{l\Gamma\left(n+1\right)}G_{1,[1:1],\,0,\,[1:1]}^{1,\,1,\,1,\,1,\,1}\left(\begin{matrix}\frac{\overline{\gamma_1}}{i}\\ \frac{\overline{\gamma_2}}{l}\end{matrix}\middle|\begin{matrix}2\\ -k;\,-n\\ -\\ 0;\,0\end{matrix}\right), \tag{32}$$

$$C \geq \frac{1}{\ln 2}\sum_{i=1}^{s_1}\sum_{j=t_1-s_1}^{(t_1+s_1-2i)i}\sum_{k=0}^{j} d_1\left(i,\, j\right) e^{\frac{i}{\overline{\gamma_1}}}\mathrm{E}_{1+k}\left(\frac{i}{\overline{\gamma_1}}\right) + \frac{1}{\ln 2}\sum_{l=1}^{s_2}\sum_{m=t_2-s_2}^{(t_2+s_2-2l)l}\sum_{n=0}^{m} d_2\left(l,\, m\right) e^{\frac{l}{\overline{\gamma_2}}}\mathrm{E}_{1+n}\left(\frac{l}{\overline{\gamma_2}}\right)$$
$$- \log_2\left(1 + \overline{\gamma_1}\sum_{i=1}^{s_1}\sum_{j=t_1-s_1}^{(t_1+s_1-2i)i}\frac{d_1\left(i,\, j\right)}{j!}\frac{1}{i}\Gamma\left(j+2\right) + \overline{\gamma_2}\sum_{l=1}^{s_2}\sum_{m=t_2-s_2}^{(t_2+s_2-2l)l}\frac{d_2\left(l,\, m\right)}{m!}\frac{1}{l}\Gamma\left(m+2\right)\right), \tag{35}$$

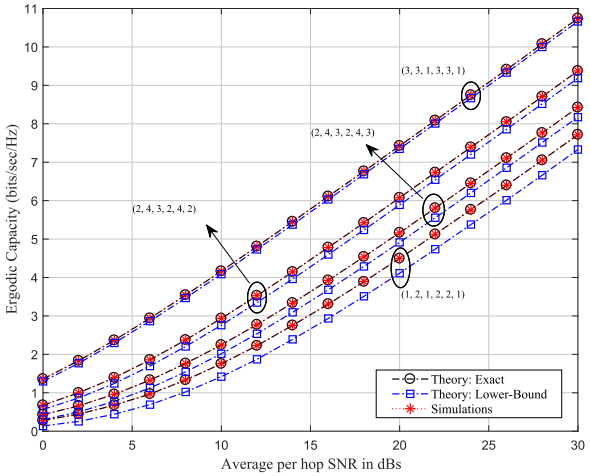

Fig. 3. Multi-antenna FD relaying ergodic capacity against the first-hop SNR ($\overline{\gamma_1}$) where $\overline{\gamma_1} = \overline{\gamma_2}$, for different settings $(N_S,\ N_R,\ M_R,\ N_T,\ N_D,\ M_D)$.

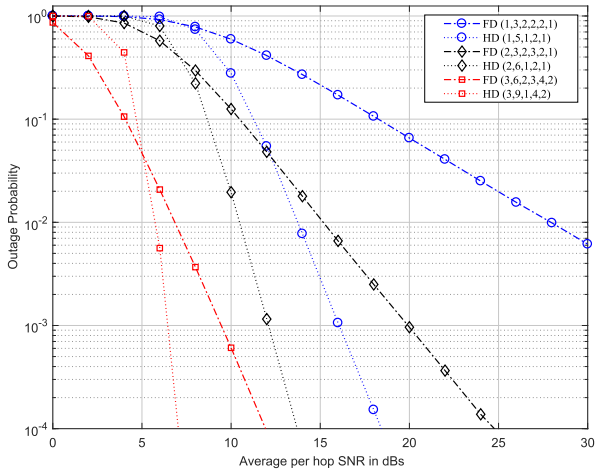

Fig. 4. Multi-antenna FD and HD relaying outage probabilities against the first-hop SNR ($\overline{\gamma_1}$) where $\overline{\gamma_1} = \overline{\gamma_2}$, with $R_0 = 2$ bits/sec/Hz, and for different settings FD $(N_S,\ N_R,\ M_R,\ N_T,\ N_D,\ M_D)$ and HD $\left(N_S,\ N_R + N_T,\ \frac{M_R}{2}, N_D,\ M_D\right)$.

that the Monte Carlo simulations and presented mathematical formulas in (32) attain an accurate coincide which corroborates the precision of the presented accurate closed-form mathematical formula. Furthermore, the closeness of the considered lower-bound mathematical formula in (35) is confirmed, where it gets closer at high array gain and/or diversity order. Our analysis reveals a significant ergodic capacity improvement as a result of higher diversity order and/or high average per-hop SNR. Meanwhile, less enhancement is noticed as a consequence of higher array gain. The harmful impact of the amount of CCI interference on the ergodic capacity performance of multi-antenna FD relaying networks is obviously noted.

Fig. 4 shows the outage probabilities of multi-antenna FD and HD relaying networks for several antenna configurations and amount of CCI interferers. We indicate the so named RF chain maintained status, hence, the HD relaying mode antennas is defined as $N = N_R + N_T$. In addition, as denoted in [1], the amount of CCI in FD mode networks is

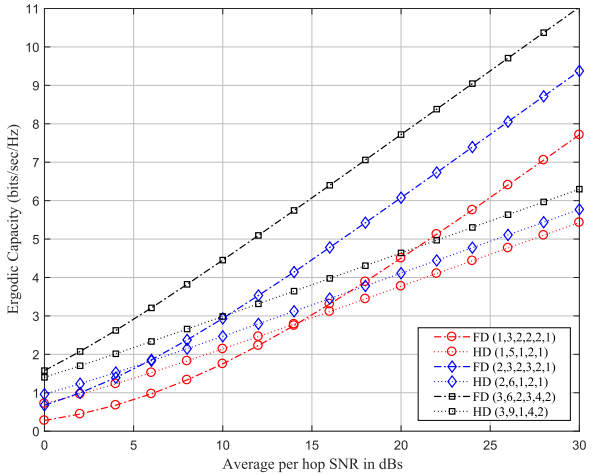

Fig. 5. Multi-antenna FD and HD relaying ergodic capacities against the first-hop SNR ($\overline{\gamma_1}$) where $\overline{\gamma_1} = \overline{\gamma_2}$, for different settings FD $(N_S,\ N_R,\ M_R,\ N_T,\ N_D,\ M_D)$ and HD $(N_S,\ N_R + N_T,\ \frac{M_R}{2},\ N_D,\ M_D)$.

doubled in contrast to its HD mode rival. It is easily observed that the multi-antenna FD relaying networks outperforms its HD relaying counterpart in terms of outage probability at low SNRs. However, at high SNRs, the outage probability of multi-antenna HD relaying networks is superior. The harmful impact of the amount of CCI interference on the outage performance of multi-antenna FD relaying modes is easily noticed.

In Fig. 5, an ergodic capacity comparison for multi-antenna FD and HD relaying networks is presented. When the diversity order is low, it is seen that the ergodic capacity of multi-antenna FD relaying mode outperforms its HD relaying mode counterpart at high SNRs. However, at low SNRs, the performance of multi-antenna HD relaying is superior. The harmful impact of the amount of CCI interference on the performance of multi-antenna FD relaying networks is easily observed. On the other hand, when the diversity order is high, i.e., $\min\left(N_S\left(N_R - M_R\right),\ \left(N_T - 1\right)\left(N_D - M_D\right)\right)$ is high, the performance of multi-antenna FD relaying mode outperforms its HD relaying mode rival at every SNR regime.

Fig. 6 shows comparisons between the ergodic capacity of ZF and MRT beamforming schemes under different levels of loopback self interference variances σ_R^2 and co-channel interfernce-to-noise ratio ρ_I. It is clearly seen that at very low σ_R^2 and ρ_I, the ergodic capacity of MRT beamforming outperforms that of the ZF beamforming at low SNRs, while at high SNRs, the oppsite is true. Meanwhile, once σ_R^2 and/or ρ_I starts to increase, the ergodic capacity of ZF beamfoming surpasses that of the MRT beamforming. In addition, a ceiling effect is observed in the case of MRT beamforming at high SNRs regardless of the strength of σ_R^2 and ρ_I. Moreover, σ_R^2 has a stronger impact on the performance as its effect is linearly proportional to the relay transmit power, resulting in a ceiling with worse performance. Therefore, in the presence of moderate to high σ_R^2 and/or ρ_I, the performance of ZF beamfoming always performs better than MRT beamforming. Note that ZF beamforming is the same regardless of the interference levels σ_R^2 and ρ_I as it uses null space projections to transmit

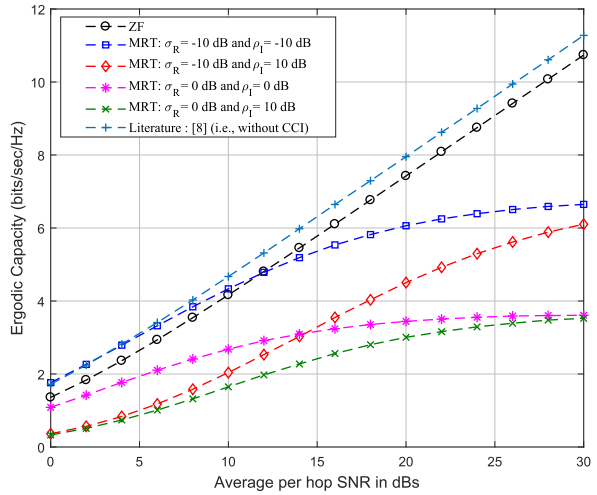

Fig. 6. Comparison between the ergodic capacities of ZF and MRT beamforming against the first-hop SNR ($\overline{\gamma_1}$) where $\overline{\gamma_1} = \overline{\gamma_2}$, for the system settings (3, 3, 1, 3, 3, 1), and with differnt loopback self interference variance σ_R^2 and co-channel interfernce-to-noise ratio values, when $\rho_i^R = \rho_i^D = \rho_I$.

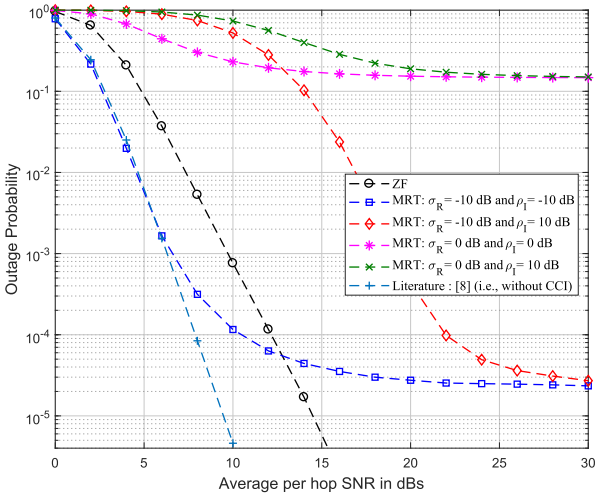

Fig. 7. Comparison between the outage probabilities of ZF and MRT beamforming against the first-hop SNR ($\overline{\gamma_1}$) where $\overline{\gamma_1} = \overline{\gamma_2}$, for the system settings (3, 3, 1, 3, 3, 1), with $R_0 = 2$ bits/sec/Hz, and for differnt loopback self interference variance σ_R^2 and co-channel interfernce-to-noise ratio values, when $\rho_i^R = \rho_i^D = \rho_I$.

and receive in orthogonal spaces to the interferers through the proposed orthogonally projected channels. Meanwhile, for comparison purposes, an ergodic capacity upper-bound from the literature has been included in Fig. 6, where the impact of CCI has been ignored.[9] Therefore, the literature settings in this case is simply (3, 3, 0, 3, 3, 0).

Fig. 7 presents comparisons between the outage probabilities of ZF and MRT beamforming schemes under different levels of σ_R^2 and ρ_I. Similarly, at very low σ_R^2 and ρ_I, it is shown that the outage performance of MRT beamforming outperforms that of the ZF beamforming at low SNRs, while at high SNRs, the opposite is true. Meanwhile, once σ_R^2 and/or ρ_I starts to increase, the outage performance of ZF beamfoming exceeds that of the MRT beamforming. In addition, the outage performance of MRT beamforming reaches an error floor at high SNRs regardless of the strength of σ_R^2 and ρ_I. Furthermore, σ_R^2 has a more adverse impact on the outage performance compared to the effect of ρ_I as it controls the error floors at high SNRs resulting in a worse outage performance. On the other hand, the outage performance of ZF beamfoming is the same regardless of the interference levels σ_R^2 and ρ_I, and improves without bound with SNR. Note also here that an outage probability lower-bound from the literature has been introduced in Fig. 7.

[9]To our best knowledge, the effect of CCI at the relay and destination on the performance of MIMO full duplex relaying has not been investigated yet. However, the performance of MIMO full duplex relaying in the absence of CCI at the relay and destination has been analyzed in [8].

VII. Conclusions

In this paper, the performance of full-duplex relaying systems with multiple antenna terminals, LI and CCI has been investigated, where hop-by-hop transmit/receive ZF beamforming/combining based on null space projection was proposed so as to maximize the overall SINR and suppress the LI and CCI at the relay and destination. Exact analytical formulas for the outage probability and ergodic capacity were attained in closed-form. In addition, simpler outage probability and ergodic capacity lower-bound expressions were also introduced, through which the asymptotic outage expression was presented to explicitly reveal insights such as the achievable diversity order and array gain. These expressions yield an efficient ways for the assessment of the outage probability and ergodic capacity of the considered MIMO FD relaying systems with LI and CCI. Therefore, the influence of key system parameters such as the number of antennas at each terminal, loopback self-interference at the relay, the number of CCI interferers at the relay and destination, and the source and relay average transmit power on the system performance were investigated. Our analysis reveals that although the number of co-channel interferers is doubled in full-duplex relaying systems compared to the conventional half-duplex relaying systems, full-duplex relaying can significantly improve the system performance. The proposed theoretical framework provides useful guidelines for practical implementation of MIMO relaying systems.

Appendix A
Proof of Equation (6)

Due to the independence between the transmitted signal $x_S[n]$, the i^{th} interference signal $x_i[n]$, and the AWGN noise $\boldsymbol{n}_R[n]$, from (4), the relay transmit power is expressed as[10]

$$\begin{aligned}
&\mathbb{E}\left(|x_R[n]|^2\right) \\
&= \mathcal{G}^2 \sum_{j=0}^{\infty} \left(\left|\boldsymbol{w}_R^\dagger \boldsymbol{H}_R \boldsymbol{w}_T\right|^2 \mathcal{G}^2\right)^j \\
&\quad \times \left(\mathcal{E}_S \left|\boldsymbol{w}_R^\dagger \boldsymbol{H}_1 \boldsymbol{w}_S\right|^2 + \sum_{i=1}^{M_R} \left|\boldsymbol{w}_R^\dagger \boldsymbol{h}_i\right|^2 \mathcal{E}_i^R + \sigma^2\right) \\
&= \mathcal{G}^2 \frac{\mathcal{E}_S \left|\boldsymbol{w}_R^\dagger \boldsymbol{H}_1 \boldsymbol{w}_S\right|^2 + \sum_{i=1}^{M_R} \left|\boldsymbol{w}_R^\dagger \boldsymbol{h}_i\right|^2 \mathcal{E}_i^R + \sigma^2}{1 - \left|\boldsymbol{w}_R^\dagger \boldsymbol{H}_R \boldsymbol{w}_T\right|^2 \mathcal{G}^2},
\end{aligned} \tag{36}$$

[10]Similar derivations for the case of single antenna nodes could be found in [40].

where the well known geometric series $\sum_{j=0}^{\infty}\alpha\,(x)^j = \frac{\alpha}{1-x}$, for $|x|<1$ is utilized in order to solve the summation $\sum_{j=0}^{\infty}\left(\left|\boldsymbol{w}_R^{\dagger}\boldsymbol{H}_R\boldsymbol{w}_T\right|^2\mathcal{G}^2\right)^j$. Note that from (3), it can be proved that $\left|\boldsymbol{w}_R^{\dagger}\boldsymbol{H}_R\boldsymbol{w}_T\right|^2\mathcal{G}^2<1$.

Due to independence between $x_R\,[n]$, $y_i\,[n]$, and $\boldsymbol{n}_D\,[n]$, from (5), the received power at the destination is written as

$$\begin{aligned}
&\mathbb{E}\left(|z_D\,[n]|^2\right)\\
&=\left|\boldsymbol{w}_D^{\dagger}\boldsymbol{H}_2\boldsymbol{w}_T\right|^2\mathbb{E}\left(|x_R\,[n]|^2\right)+I_D\\
&=\left|\boldsymbol{w}_D^{\dagger}\boldsymbol{H}_2\boldsymbol{w}_T\right|^2\mathcal{G}^2\frac{\mathcal{E}_S\left|\boldsymbol{w}_R^{\dagger}\boldsymbol{H}_1\boldsymbol{w}_S\right|^2+I_R}{1-\left|\boldsymbol{w}_R^{\dagger}\boldsymbol{H}_R\boldsymbol{w}_T\right|^2\mathcal{G}^2}+I_D\\
&=\left|\boldsymbol{w}_D^{\dagger}\boldsymbol{H}_2\boldsymbol{w}_T\right|^2\mathcal{G}^2\mathcal{E}_S\left|\boldsymbol{w}_R^{\dagger}\boldsymbol{H}_1\boldsymbol{w}_S\right|^2+\left|\boldsymbol{w}_D^{\dagger}\boldsymbol{H}_2\boldsymbol{w}_T\right|^2\mathcal{G}^2\\
&\quad\times\frac{\mathcal{E}_S\left|\boldsymbol{w}_R^{\dagger}\boldsymbol{H}_1\boldsymbol{w}_S\right|^2\left|\boldsymbol{w}_R^{\dagger}\boldsymbol{H}_R\boldsymbol{w}_T\right|^2\mathcal{G}^2+I_R}{1-\left|\boldsymbol{w}_R^{\dagger}\boldsymbol{H}_R\boldsymbol{w}_T\right|^2\mathcal{G}^2}+I_D, \quad (37)
\end{aligned}$$

where $I_R=\sum_{i=1}^{M_R}\left|\boldsymbol{w}_R^{\dagger}\boldsymbol{h}_i\right|^2\mathcal{E}_i^R+\sigma^2$ and $I_D=\sum_{i=1}^{M_D}\left|\boldsymbol{w}_D^{\dagger}\boldsymbol{g}_i\right|^2\mathcal{E}_i^D+\sigma^2$.

Upon reforming (37) into a sum of desired signal power, loopback self interfernce power, co-channel interefernce powers, and noise powers, we arrive at

$$\begin{aligned}
&\mathbb{E}\left(|z_D\,[n]|^2\right)\\
&=\left|\boldsymbol{w}_D^{\dagger}\boldsymbol{H}_2\boldsymbol{w}_T\right|^2\mathcal{G}^2\mathcal{E}_S\left|\boldsymbol{w}_R^{\dagger}\boldsymbol{H}_1\boldsymbol{w}_S\right|^2\\
&\quad+\left|\boldsymbol{w}_D^{\dagger}\boldsymbol{H}_2\boldsymbol{w}_T\right|^2\mathcal{G}^2I_R+\left|\boldsymbol{w}_D^{\dagger}\boldsymbol{H}_2\boldsymbol{w}_T\right|^2\mathcal{G}^2\\
&\quad\times\frac{\mathcal{E}_S\left|\boldsymbol{w}_R^{\dagger}\boldsymbol{H}_1\boldsymbol{w}_S\right|^2\left|\boldsymbol{w}_R^{\dagger}\boldsymbol{H}_R\boldsymbol{w}_T\right|^2\mathcal{G}^2+I_R\left|\boldsymbol{w}_R^{\dagger}\boldsymbol{H}_R\boldsymbol{w}_T\right|^2\mathcal{G}^2}{1-\left|\boldsymbol{w}_R^{\dagger}\boldsymbol{H}_R\boldsymbol{w}_T\right|^2\mathcal{G}^2}\\
&\quad+I_D. \quad (38)
\end{aligned}$$

Therefore, from (38), the instantanous overall SINR may be expressed as in (39), as shown at the top of next page, which upon substituting the relay gain from (3) into (39), reduces to (40), as shown at the top of next page,

Hence, once dividing the numerator and denominator by $I_D\left(\mathcal{E}_R\left|\boldsymbol{w}_R^{\dagger}\boldsymbol{H}_R\boldsymbol{w}_T\right|^2+I_R\right)$ and substituting back $I_R=\sum_{i=1}^{M_R}\left|\boldsymbol{w}_R^{\dagger}\boldsymbol{h}_i\right|^2\mathcal{E}_i^R+\sigma^2$ and $I_D=\sum_{i=1}^{M_D}\left|\boldsymbol{w}_D^{\dagger}\boldsymbol{g}_i\right|^2\mathcal{E}_i^D+\sigma^2$ into (40), we arrive at (6), that concludes the proof.

Appendix B
Proof of Proposition 1

In order to find an explicit expression for the optimal solution to the optimization problem in (10), the required solution according to the MRC principle may be expressed in the following form $\boldsymbol{w}_R=\frac{\boldsymbol{P}\boldsymbol{H}_1\boldsymbol{w}_S}{\|\boldsymbol{P}\boldsymbol{H}_1\boldsymbol{w}_S\|}$, here, the two constraints are incorporated in this preferable formula, namely, 1) the projection matrix $\boldsymbol{P}$ which assures that $\boldsymbol{w}_R\perp\boldsymbol{H}$ (owing to the fact that $\boldsymbol{H}^{\dagger}\boldsymbol{w}_R=0$), where, $\boldsymbol{P}=\boldsymbol{I}_{N_R}-\boldsymbol{H}\left(\boldsymbol{H}^{\dagger}\boldsymbol{H}\right)^{-1}\boldsymbol{H}^{\dagger}$, 2) the division by $\|\boldsymbol{P}\boldsymbol{H}_1\boldsymbol{w}_S\|$ assures that the norm of $\boldsymbol{w}_R$ equals one, $\|\boldsymbol{w}_R\|=1$. Therefore, (10) can be re-written as

$$\begin{aligned}
\boldsymbol{w}_S^{\star}=&\arg\max_{\boldsymbol{w}_S}\ \|\boldsymbol{P}\boldsymbol{H}_1\boldsymbol{w}_S\|^2\\
&\text{subject to }\ \|\boldsymbol{w}_S\|=1. \quad (41)
\end{aligned}$$

This is a well known problem (known as the squared spectral norm) and its optimal solution is $\boldsymbol{w}_S^{\star}=\boldsymbol{u}_{\max}\left(\boldsymbol{H}_1^{\dagger}\boldsymbol{P}\boldsymbol{H}_1\right)$, the eigenvector corresponds to the largest eigenvalue of the matrix $\boldsymbol{H}_1^{\dagger}\boldsymbol{P}\boldsymbol{H}_1$, termed as $\lambda_{\max}\left(\boldsymbol{H}_1^{\dagger}\boldsymbol{P}\boldsymbol{H}_1\right)$, where $\|\boldsymbol{P}\boldsymbol{H}_1\boldsymbol{w}_S^{\star}\|^2=\lambda_{\max}\left(\boldsymbol{H}_1^{\dagger}\boldsymbol{P}\boldsymbol{H}_1\right)=\|\boldsymbol{P}\boldsymbol{H}_1\|_2^2$.

Similarly for (11), let $\boldsymbol{w}_D=\frac{\boldsymbol{B}\boldsymbol{H}_2\boldsymbol{w}_T}{\|\boldsymbol{B}\boldsymbol{H}_2\boldsymbol{w}_T\|}$, hence

$$\begin{aligned}
\boldsymbol{w}_T^{\star}=&\arg\max_{\boldsymbol{w}_T}\ \|\boldsymbol{B}\boldsymbol{H}_2\boldsymbol{w}_T\|^2\\
&\text{s. t. }\boldsymbol{w}_S^{\star\dagger}\boldsymbol{H}_1^{\dagger}\boldsymbol{P}\boldsymbol{H}_R\boldsymbol{w}_T=0\ \&\ \|\boldsymbol{w}_T\|=1, \quad (42)
\end{aligned}$$

where $\boldsymbol{B}=\boldsymbol{I}_{N_D}-\boldsymbol{G}\left(\boldsymbol{G}^{\dagger}\boldsymbol{G}\right)^{-1}\boldsymbol{G}^{\dagger}$. The needed result could be formulated in the upcoming layout $\boldsymbol{w}_T=\boldsymbol{D}\boldsymbol{z}$, hence, (42) can be reformed as[11]

$$\begin{aligned}
\boldsymbol{z}^{\star}=&\arg\max_{\boldsymbol{z}}\ \|\boldsymbol{B}\boldsymbol{H}_2\boldsymbol{D}\boldsymbol{z}\|^2\\
&\text{s. t. }\ \|\boldsymbol{D}\boldsymbol{z}\|=1, \quad (43)
\end{aligned}$$

where $\boldsymbol{D}=\boldsymbol{I}_{N_T}-\frac{\boldsymbol{H}_R^{\dagger}\boldsymbol{P}\boldsymbol{H}_1\boldsymbol{w}_S^{\star}\left(\boldsymbol{H}_R^{\dagger}\boldsymbol{P}\boldsymbol{H}_1\boldsymbol{w}_S^{\star}\right)^{\dagger}}{\left(\boldsymbol{H}_R^{\dagger}\boldsymbol{P}\boldsymbol{H}_1\boldsymbol{w}_S^{\star}\right)^{\dagger}\boldsymbol{H}_R^{\dagger}\boldsymbol{P}\boldsymbol{H}_1\boldsymbol{w}_S^{\star}}$. Similar to (41), the optimal solution for (43) is $\boldsymbol{z}^{\star}=\frac{\boldsymbol{u}_{\max}\left(\boldsymbol{D}\boldsymbol{H}_2^{\dagger}\boldsymbol{B}\boldsymbol{H}_2\boldsymbol{D}\right)}{\left\|\boldsymbol{D}\boldsymbol{u}_{\max}\left(\boldsymbol{D}\boldsymbol{H}_2^{\dagger}\boldsymbol{B}\boldsymbol{H}_2\boldsymbol{D}\right)\right\|}$, where $\|\boldsymbol{B}\boldsymbol{H}_2\boldsymbol{D}\boldsymbol{z}^{\star}\|^2=\lambda_{\max}\left(\boldsymbol{D}\boldsymbol{H}_2^{\dagger}\boldsymbol{B}\boldsymbol{H}_2\boldsymbol{D}\right)=\|\boldsymbol{B}\boldsymbol{H}_2\boldsymbol{D}\|_2^2$.

Appendix C
Proof of Proposition 2

Substituting (18) and (19) into (24) yields (44), shown at the top of next page.

Applying the binomial expansion $(A+B)^N=\sum_{n=0}^{N}\binom{N}{n}A^{N-n}B^n$, equation (44) reduces to (45), as shown at the top of next page.

The integral I_1 is attained by using [37, eq. (3.471.9)], which upon substituting I_1 into (45), results in (25), this finishes the proof.

[11] Alternatively, one could choose $\boldsymbol{w}_T$ as $\boldsymbol{w}_T=\frac{\boldsymbol{D}\boldsymbol{z}}{\|\boldsymbol{D}\boldsymbol{z}\|}$, in this case, $\boldsymbol{z}^{\star}=\arg\max_{\boldsymbol{z}}\ \frac{\|\boldsymbol{B}\boldsymbol{H}_2\boldsymbol{D}\boldsymbol{z}\|^2}{\|\boldsymbol{D}\boldsymbol{z}\|^2}$. Hence, by utilizing Cauchy–Schwarz inequality; $\|\boldsymbol{B}\boldsymbol{H}_2\boldsymbol{D}\boldsymbol{z}\|^2\le\|\boldsymbol{B}\boldsymbol{H}_2\boldsymbol{D}\|_2^2\,\|\boldsymbol{D}\boldsymbol{z}\|^2$, similar results could be derived.

$$\gamma = \frac{\mathcal{E}_S \left|\boldsymbol{w}_R^\dagger \boldsymbol{H}_1 \boldsymbol{w}_S\right|^2 \left|\boldsymbol{w}_D^\dagger \boldsymbol{H}_2 \boldsymbol{w}_T\right|^2}{\left|\boldsymbol{w}_D^\dagger \boldsymbol{H}_2 \boldsymbol{w}_T\right|^2 \left(I_R + \frac{\left(\mathcal{E}_S \left|\boldsymbol{w}_R^\dagger \boldsymbol{H}_1 \boldsymbol{w}_S\right|^2 + I_R\right) \left|\boldsymbol{w}_R^\dagger \boldsymbol{H}_R \boldsymbol{w}_T\right|^2}{\frac{1}{\mathcal{G}^2} - \left|\boldsymbol{w}_R^\dagger \boldsymbol{H}_R \boldsymbol{w}_T\right|^2}\right) + \frac{I_D}{\mathcal{G}^2}}. \tag{39}$$

$$\gamma = \frac{\mathcal{E}_S \left|\boldsymbol{w}_R^\dagger \boldsymbol{H}_1 \boldsymbol{w}_S\right|^2 \mathcal{E}_R \left|\boldsymbol{w}_D^\dagger \boldsymbol{H}_2 \boldsymbol{w}_T\right|^2}{\mathcal{E}_S \left|\boldsymbol{w}_R^\dagger \boldsymbol{H}_1 \boldsymbol{w}_S\right|^2 I_D + \mathcal{E}_R \left|\boldsymbol{w}_D^\dagger \boldsymbol{H}_2 \boldsymbol{w}_T\right|^2 \left(\mathcal{E}_R \left|\boldsymbol{w}_R^\dagger \boldsymbol{H}_R \boldsymbol{w}_T\right|^2 + I_R\right) + I_D \left(\mathcal{E}_R \left|\boldsymbol{w}_R^\dagger \boldsymbol{H}_R \boldsymbol{w}_T\right|^2 + I_R\right)}. \tag{40}$$

$$F_\gamma(\gamma_T) = 1 - \sum_{i=1}^{s_1} \sum_{j=t_1-s_1}^{(t_1+s_1-2i)i} \sum_{k=0}^{j} \frac{i^k d_1(i,j)}{k! \overline{\gamma_1}^k} \gamma_T^k e^{-i\frac{\gamma_T}{\overline{\gamma_1}}} \sum_{l=1}^{s_2} \sum_{m=t_2-s_2}^{(t_2+s_2-2l)l} \frac{l^{m+1} d_2(l,m)}{m! \overline{\gamma_2}^{m+1}} e^{-\frac{l\gamma_T}{\overline{\gamma_2}}} \times \int_0^\infty w^{-k} (\gamma_T + 1 + w)^k e^{-i\frac{\gamma_T(\gamma_T+1)}{\overline{\gamma_1} w} - \frac{lw}{\overline{\gamma_2}}} (\gamma_T + w)^m dw. \tag{44}$$

$$F_\gamma(\gamma_T) = 1 - \sum_{i=1}^{s_1} \sum_{j=t_1-s_1}^{(t_1+s_1-2i)i} \sum_{k=0}^{j} \frac{i^k d_1(i,j)}{k! \overline{\gamma_1}^k} \gamma_T^k e^{-i\frac{\gamma_T}{\overline{\gamma_1}}} \sum_{p=0}^{k} \binom{k}{p} (\gamma_T + 1)^p \sum_{l=1}^{s_2} \sum_{m=t_2-s_2}^{(t_2+s_2-2l)l} \times \frac{l^{m+1} d_2(l,m)}{m! \overline{\gamma_2}^{m+1}} e^{-\frac{l\gamma_T}{\overline{\gamma_2}}} \sum_{n=0}^{m} \binom{m}{n} \gamma_T^{m-n} \underbrace{\int_0^\infty w^{n-p} e^{-i\frac{\gamma_T(\gamma_T+1)}{\overline{\gamma_1} w} - \frac{lw}{\overline{\gamma_2}}} dw}_{I_1}. \tag{45}$$

Appendix D
Proof of Equation (27)

Given the overall SINR bound (26), then

$$\begin{aligned} &F_{\gamma_{\text{up}}}(\gamma_T) \\ &= \Pr(\min(\gamma_1, \gamma_2) < \gamma_T) \\ &= 1 - (1 - F_{\gamma_1}(\gamma_T))(1 - F_{\gamma_2}(\gamma_T)) \\ &= 1 - \sum_{i=1}^{s_1} \sum_{j=t_1-s_1}^{(t_1+s_1-2i)i} d_1(i,j) e^{-\frac{i\gamma_T}{\overline{\gamma_1}}} \sum_{k=0}^{j} \frac{\left(\frac{i\gamma_T}{\overline{\gamma_1}}\right)^k}{k!} \\ &\quad \times \sum_{l=1}^{s_2} \sum_{m=t_2-s_2}^{(t_2+s_2-2l)l} d_2(l,m) e^{-\frac{l\gamma_T}{\overline{\gamma_2}}} \sum_{n=0}^{m} \frac{\left(\frac{l\gamma_T}{\overline{\gamma_2}}\right)^n}{n!}. \end{aligned} \tag{46}$$

Upon substituting the CDF of γ_1 and γ_2 and utilizing [37, eq. (8.352.4)], (46) simplifies to (27), that finishes the proof.

Appendix E
Proof of Equation (28)

The asymptotic approximations could be attained by tackling the approximate expansion of the incomplete gamma function [37, eq. (8.354.1)]. Hence, upon using the asymptotic results of the CDF of the $\boldsymbol{S} \rightarrow \boldsymbol{R}$ and $\boldsymbol{R} \rightarrow \boldsymbol{D}$ links [41, eq. (27)], equation (46) reduces to

$$\begin{aligned} &F_\gamma^\infty(\gamma_T) \\ &= 1 - \left(1 - \frac{\prod_{l=0}^{s_1-1} l!}{\prod_{l=0}^{s_1-1} (t_1 + l)!} \left(\frac{\gamma_T}{\overline{\gamma_1}}\right)^{N_S(N_R-M_R)}\right) \\ &\quad \times \left(1 - \frac{\prod_{l=0}^{s_2-1} l!}{\prod_{l=0}^{s_2-1} (t_2 + l)!} \left(\frac{\gamma_T}{\overline{\gamma_2}}\right)^{(N_T-1)(N_D-M_D)}\right). \end{aligned} \tag{47}$$

To this end, simplifying (47) yields (28), that finishes the proof.

Appendix F
Proof of Proposition 4

To get a closed-form formula to (29), it is more appropriate to utilize another formula for the MGF term obtained in (31). Therefore, given the CDF of γ_i in (18), an appropriate formula for the MGF in (31) could be given as [26, eq. (45)]

$$\mathcal{M}_{\gamma_i}(z) = z \int_0^\infty e^{-z\gamma_i} F_{\gamma_i}(\gamma) d\gamma. \tag{48}$$

Hence,

$$\mathcal{M}_{\gamma_1}(z) = 1 - \overline{\gamma_1} \sum_{i=1}^{s_1} \sum_{j=t_1-s_1}^{(t_1+s_1-2i)i} \sum_{k=0}^{j} \frac{d_1(i,j)}{i} \frac{z}{\left(\frac{\overline{\gamma_1}}{i} z + 1\right)^{k+1}}, \tag{49}$$

and

$$\mathcal{M}_{\gamma_2}(z) = 1 - \overline{\gamma_2} \sum_{l=1}^{s_2} \sum_{m=t_2-s_2}^{(t_2+s_2-2l)l} \sum_{n=0}^{m} \frac{d_2(l,m)}{l} \times \frac{z}{\left(\frac{\overline{\gamma_2}}{l} z + 1\right)^{n+1}}. \tag{50}$$

From (29)-(30), the ergodic capacity can be defined as

$$\begin{aligned} C &= \frac{1}{\ln 2} \mathbb{E}\left[\ln\left(1 + \frac{\gamma_1 \gamma_2}{\gamma_1 + \gamma_2 + 1}\right)\right] \\ &= \frac{1}{\ln 2} \int_0^\infty \frac{1}{z} (1 - \mathcal{M}_{\gamma_1}(z))(1 - \mathcal{M}_{\gamma_2}(z)) e^{-z} dz. \end{aligned} \tag{51}$$

Substituting $\mathcal{M}_{\gamma_1}(z)$ and $\mathcal{M}_{\gamma_2}(z)$ from (49) and (50) into (51), we have

$$C = \frac{\overline{\gamma_1}\,\overline{\gamma_2}}{\ln 2}\sum_{i=1}^{s_1}\sum_{j=t_1-s_1}^{(t_1+s_1-2i)i}\sum_{k=0}^{j}\frac{d_1(i,j)}{i} \times\sum_{l=1}^{s_2}\sum_{m=t_2-s_2}^{(t_2+s_2-2l)l}\sum_{n=0}^{m}\frac{d_2(l,m)}{l} \times\underbrace{\int_0^{\infty} z\frac{1}{\left(\frac{\overline{\gamma_1}}{i}z+1\right)^{k+1}}\frac{1}{\left(\frac{\overline{\gamma_2}}{l}z+1\right)^{n+1}}e^{-z}dz}_{I_2}. \quad (52)$$

Since

$$\left(\frac{1}{1+\lambda x}\right)^{\alpha} = \frac{1}{\Gamma(\alpha)}G_{1,1}^{1,1}\left(\lambda x\left|\begin{matrix}1-\alpha\\0\end{matrix}\right.\right), \quad (53)$$

the integral I_2 in (52) can be simplified to

$$I_2 = \frac{1}{\Gamma(k+1)}\frac{1}{\Gamma(n+1)} \times\underbrace{\int_0^{\infty} z\,G_{1,1}^{1,1}\left(\frac{\overline{\gamma_1}}{i}z\left|\begin{matrix}-k\\0\end{matrix}\right.\right)G_{1,1}^{1,1}\left(\frac{\overline{\gamma_2}}{l}z\left|\begin{matrix}-n\\0\end{matrix}\right.\right)e^{-z}dz}_{I_3}. \quad (54)$$

The integral I_3 can be simplified by utilizing [42, eq. (2.6.2)], resulting in

$$I_2 = \frac{1}{\Gamma(k+1)}\frac{1}{\Gamma(n+1)}G_{1,[1:1],0,[1:1]}^{1,1,1,1,1}\left(\begin{matrix}\frac{\overline{\gamma_1}}{i}\\ \frac{\overline{\gamma_2}}{l}\end{matrix}\left|\begin{matrix}2\\-k;\,-n\\-\\0;\,0\end{matrix}\right.\right). \quad (55)$$

Hence, substituting (55) into (52) yields (32), that finishes the proof.

Appendix G
Proof of Equation (35)

The evaluation of $C_{\gamma_i} = \mathbb{E}[\log_2(1+\gamma_i)] = \frac{1}{\ln 2}\mathbb{E}[\ln(1+\gamma_i)]$ can be conducted by utilizing [43, Lemma 1] which says, for any $\gamma_i \geq 0$, we have

$$\mathbb{E}[\ln(1+\gamma_i)] = \int_0^{\infty}\frac{1}{z}\left(1-\mathcal{M}_{\gamma_i}(z)\right)e^{-z}dz, \quad (56)$$

where $\mathcal{M}_{\gamma_i}(z) = \mathbb{E}[e^{-z\gamma_i}]$, $i \in \{1,2\}$ and are given in (49) and (50).

Substituting the MGFs from (49) into (56), we obtain

$$C_{\gamma_1} = \frac{\overline{\gamma_1}}{\ln 2}\sum_{i=1}^{s_1}\sum_{j=t_1-s_1}^{(t_1+s_1-2i)i}\sum_{k=0}^{j}\frac{d_1(i,j)}{i} \times\underbrace{\int_0^{\infty}\frac{1}{\left(\frac{\overline{\gamma_1}}{i}z+1\right)^{k+1}}e^{-z}dz}_{I_4}. \quad (57)$$

The integral I_4 is attained by using [37, eq. (9.211.4)], resulting in

$$C_{\gamma_1} = \frac{1}{\ln 2}\sum_{i=1}^{s_1}\sum_{j=t_1-s_1}^{(t_1+s_1-2i)i}\sum_{k=0}^{j}d_1(i,j)\,\Psi\left(1,1-k;\frac{i}{\overline{\gamma_1}}\right). \quad (58)$$

Utilizing the fact that $\Psi\left(1,1-k;\frac{i}{\overline{\gamma_1}}\right) = e^{\frac{i}{\overline{\gamma_1}}}\mathrm{E}_{1+k}\left(\frac{i}{\overline{\gamma_1}}\right)$, (58) reduces to

$$C_{\gamma_1} = \frac{1}{\ln 2}\sum_{i=1}^{s_1}\sum_{j=t_1-s_1}^{(t_1+s_1-2i)i}\sum_{k=0}^{j}d_1(i,j)\,e^{\frac{i}{\overline{\gamma_1}}}\mathrm{E}_{1+k}\left(\frac{i}{\overline{\gamma_1}}\right). \quad (59)$$

Similarly,

$$C_{\gamma_2} = \frac{1}{\ln 2}\sum_{l=1}^{s_2}\sum_{m=t_2-s_2}^{(t_2+s_2-2l)l}\sum_{n=0}^{m}d_2(l,m)\,e^{\frac{l}{\overline{\gamma_2}}}\mathrm{E}_{1+n}\left(\frac{l}{\overline{\gamma_2}}\right). \quad (60)$$

The averages in (34) may be obtained straightforward by using [37, eq. (3.381.4)], as follows

$$\begin{aligned}\mathbb{E}\left[\overline{\gamma_1}\|\boldsymbol{P}\boldsymbol{H}_1\|_2^2\right] &= \overline{\gamma_1}\sum_{i=1}^{s_1}\sum_{j=t_1-s_1}^{(t_1+s_1-2i)i}\frac{i^{j+1}d_1(i,j)}{j!}\int_0^{\infty}x^{j+1}e^{-ix}dx\\ &= \overline{\gamma_1}\sum_{i=1}^{s_1}\sum_{j=t_1-s_1}^{(t_1+s_1-2i)i}\frac{d_1(i,j)}{j!}\frac{1}{i}\Gamma(j+2), \end{aligned} \quad (61)$$

and

$$\begin{aligned}\mathbb{E}\left[\overline{\gamma_2}\|\boldsymbol{B}\boldsymbol{H}_2\boldsymbol{D}\|_2^2\right] &= \overline{\gamma_2}\sum_{l=1}^{s_2}\sum_{m=t_2-s_2}^{(t_2+s_2-2l)l}\frac{l^{m+1}d_2(l,m)}{m!\overline{\gamma_2}^{m+1}}\int_0^{\infty}y^{m+1}e^{-\frac{ly}{\overline{\gamma_2}}}dy\\ &= \overline{\gamma_2}\sum_{l=1}^{s_2}\sum_{m=t_2-s_2}^{(t_2+s_2-2l)l}\frac{d_2(l,m)}{m!}\frac{1}{l}\Gamma(m+2). \end{aligned} \quad (62)$$

Acknowledgment

The authors would like to acknowledge the support of the University of Surrey 5GIC (http://www.surrey.ac.uk/5gic) members for this work.

References

[1] S. Goyal, P. Liu, S. S. Panwar, R. A. Difazio, R. Yang, and E. Bala, "Full duplex cellular systems: Will doubling interference prevent doubling capacity?" *IEEE Commun. Mag.*, vol. 53, no. 5, pp. 121–127, May 2015.

[2] D. Kim, H. Lee, and D. Hong, "A survey of in-band full-duplex transmission: From the perspective of PHY and MAC layers," *IEEE Commun. Surveys Tuts.*, vol. 17, no. 4, pp. 2017–2046, 4th Quart., 2015.

[3] Y. Liao, L. Song, Z. Han, and Y. Li, "Full duplex cognitive radio: A new design paradigm for enhancing spectrum usage," *IEEE Commun. Mag.*, vol. 53, no. 5, pp. 138–145, May 2015.

[4] G. Liu, F. R. Yu, H. Ji, V. C. M. Leung, and X. Li, "In-band full-duplex relaying: A survey, research issues and challenges," *IEEE Commun. Surveys Tuts.*, vol. 17, no. 2, pp. 500–524, 2nd Quart., 2015.

[5] A. Sabharwal, P. Schniter, D. Guo, D. W. Bliss, S. Rangarajan, and R. Wichman, "In-band full-duplex wireless: Challenges and opportunities," *IEEE J. Sel. Areas Commun.*, vol. 32, no. 9, pp. 1637–1652, Sep. 2014.

[6] H. Q. Ngo, H. A. Suraweera, M. Matthaiou, and E. G. Larsson, "Multipair full-duplex relaying with massive arrays and linear processing," *IEEE J. Sel. Areas Commun.*, vol. 32, no. 9, pp. 1721–1737, Sep. 2014.

[7] T. Riihonen, S. Werner, and R. Wichman, "Mitigation of loopback self-interference in full-duplex MIMO relays," *IEEE Trans. Signal Process.*, vol. 59, no. 12, pp. 5983–5993, Dec. 2011.

[8] H. A. Suraweera, I. Krikidis, G. Zheng, C. Yuen, and P. J. Smith, "Low-complexity end-to-end performance optimization in MIMO full-duplex relay systems," *IEEE Trans. Wireless Commun.*, vol. 13, no. 2, pp. 913–927, Feb. 2014.

[9] Z. Zhang, X. Chai, K. Long, A. V. Vasilakos, and L. Hanzo, "Full duplex techniques for 5G networks: Self-interference cancellation, protocol design, and relay selection," *IEEE Commun. Mag.*, vol. 53, no. 5, pp. 128–137, May 2015.

[10] U. Ugurlu, T. Riihonen, and R. Wichman, "Optimized in-band full-duplex MIMO relay under single-stream transmission," *IEEE Trans. Veh. Technol.*, vol. 65, no. 1, pp. 155–168, Jan. 2016.

[11] G. Zheng, "Joint beamforming optimization and power control for full-duplex MIMO two-way relay channel," *IEEE Trans. Signal Process.*, vol. 63, no. 3, pp. 555–566, Feb. 2015.

[12] M. Zhou, L. Song, Y. Li, and X. Li, "Simultaneous bidirectional link selection in full duplex MIMO systems," *IEEE Trans. Wireless Commun.*, vol. 14, no. 7, pp. 4052–4062, Jul. 2015.

[13] H. Ju, E. Oh, and D. Hong, "Improving efficiency of resource usage in two-hop full duplex relay systems based on resource sharing and interference cancellation," *IEEE Trans. Wireless Commun.*, vol. 8, no. 8, pp. 3933–3938, Aug. 2009.

[14] M. A. Ahmed, C. C. Tsimenidis, and A. F. Al Rawi, "Performance analysis of full-duplex-MRC-MIMO with self-interference cancellation using null-space-projection," *IEEE Trans. Signal Process.*, vol. 64, no. 12, pp. 3093–3105, Jun. 2016.

[15] Z. Ding, K. K. Leung, D. L. Goeckel, and D. Towsley, "On the application of cooperative transmission to secrecy communications," *IEEE J. Sel. Areas Commun.*, vol. 30, no. 2, pp. 359–368, Feb. 2012.

[16] G. Zhu, C. Zhong, H. A. Suraweera, Z. Zhang, and C. Yuen, "Outage probability of dual-hop multiple antenna AF systems with linear processing in the presence of co-channel interference," *IEEE Trans. Wireless Commun.*, vol. 13, no. 4, pp. 2308–2321, Apr. 2014.

[17] G. Zhu, C. Zhong, H. A. Suraweera, Z. Zhang, C. Yuen, and R. Yin, "Ergodic capacity comparison of different relay precoding schemes in dual-hop AF systems with co-channel interference," *IEEE Trans. Wireless Commun.*, vol. 62, no. 7, pp. 2314–2328, Jul. 2014.

[18] J. Guo *et al.*, "Performance analysis of TAS/MRC in MIMO relay systems with outdated CSI and co-channel interference," *IEEE Trans. Wireless Commun.*, vol. 13, no. 9, pp. 4848–4856, Sep. 2014.

[19] S. S. Ikki and S. Aissa, "Performance analysis of two-way amplify-and-forward relaying in the presence of co-channel interferences," *IEEE Trans. Commun.*, vol. 60, no. 4, pp. 933–939, Apr. 2012.

[20] K.-C. Lee, C.-P. Li, T.-Y. Wang, and H.-J. Li, "Performance analysis of dual-hop amplify-and-forward systems with multiple antennas and co-channel interference," *IEEE Trans. Wireless Commun.*, vol. 13, no. 6, pp. 3070–3087, Jun. 2014.

[21] M. Li, M. Lin, W.-P. Zhu, Y. Huang, K.-K. Wong, and Q. Yu, "Performance analysis of dual-hop MIMO AF relaying network with multiple interferences," *IEEE Trans. Veh. Technol.*, vol. 66, no. 2, pp. 1891–1897, Feb. 2017.

[22] I. Trigui, S. Affes, and A. Stéphenne, "Ergodic capacity of two-hop multiple antenna AF systems with co-channel interference," *IEEE Wireless Commun. Lett.*, vol. 4, no. 1, pp. 26–29, Feb. 2015.

[23] H. Alves, C. H. M. de Lima, P. H. J. Nardelli, R. D. Souza, and M. Latva-Aho, "On the average spectral efficiency of interference-limited full-duplex networks," in *Proc. IEEE CROWNCOM*, Jun. 2014, pp. 550–554.

[24] H. Alves, R. D. Souza, D. B. da Costa, and M. Latva-Aho, "Full-duplex relaying systems subject to co-channel interference and noise in nakagami-m fading," in *Proc. IEEE VTC*, May 2015, pp. 1–5.

[25] G. Sharma, P. K. Sharma, and P. Garg, "Performance analysis of full duplex relaying in multicell environment," in *Proc. Int. Conf. Adv. Comput., Commun. Inform. (ICACCI)*, Sep. 2014, pp. 2501–2505.

[26] A. Almradi and K. A. Hamdi, "MIMO full-duplex relaying in the presence of co-channel interference," *IEEE Trans. Veh. Technol.*, vol. 66, no. 6, pp. 4874–4885, Jun. 2017.

[27] A. Almradi and K. A. Hamdi, "On the outage probability of MIMO full-duplex relaying: Impact of antenna correlation and imperfect CSI," *IEEE Trans. Veh. Technol.*, vol. 66, no. 5, pp. 3957–3965, May 2017.

[28] T. Riihonen, S. Werner, and R. Wichman, "Hybrid full-duplex/half-duplex relaying with transmit power adaptation," *IEEE Trans. Wireless Commun.*, vol. 10, no. 9, pp. 3074–3085, Sep. 2011.

[29] K. S. Ahn, "Performance analysis of MIMO-MRC system in the presence of multiple interferers and noise over Rayleigh fading channels," *IEEE Trans. Wireless Commun.*, vol. 8, no. 7, pp. 3727–3735, Jul. 2009.

[30] P. A. Dighe, R. K. Mallik, and S. S. Jamuar, "Analysis of transmit-receive diversity in Rayleigh fading," *IEEE Trans. Commun.*, vol. 51, no. 4, pp. 694–703, Apr. 2003.

[31] A. Maaref and S. Aissa, "Closed-form expressions for the outage and ergodic Shannon capacity of MIMO MRC systems," *IEEE Trans. Commun.*, vol. 53, no. 7, pp. 1092–1095, Jul. 2005.

[32] A. Almradi, "On the performance of MIMO full-duplex relaying in the presence of co-channel interference," in *Proc. IEEE GLOBECOM*, Dec. 2016, pp. 1–7.

[33] B. Clerckx and C. Oestges, *MIMO Wireless Networks: Channels, Techniques and Standards for Multi-Antenna, Multi-User and Multi-Cell Systems*, 2nd ed. New York, NY, USA: Academic, 2013.

[34] G. Amarasuriya, C. Tellambura, and M. Ardakani, "Performance analysis of hop-by-hop beamforming for dual-hop MIMO AF relay networks," *IEEE Trans. Commun.*, vol. 60, no. 7, pp. 1823–1837, Jul. 2012.

[35] A. Almradi and K. A. Hamdi, "The performance of wireless powered MIMO relaying with energy beamforming," *IEEE Trans. Commun.*, vol. 64, no. 11, pp. 4550–4562, Nov. 2016.

[36] M. O. Hasna and M. S. Alouini, "End-to-end performance of transmission systems with relays over Rayleigh-fading channels," *IEEE Trans. Wireless Commun.*, vol. 2, no. 6, pp. 1126–1131, Nov. 2003.

[37] I. S. Gradshteyn and I. M. Ryzhik, *Table of Integrals, Series, and Products*, 6th ed. San Diego, CA, USA: Academic, 2000.

[38] I. S. Ansari, S. Al-Ahmadi, F. Yilmaz, M.-S. Alouini, and H. Yanikomeroglu, "A new formula for the BER of binary modulations with dual-branch selection over generalized-K composite fading channels," *IEEE Trans. Commun.*, vol. 59, no. 10, pp. 2654–2658, Oct. 2011.

[39] M. Abramowitz and I. A. Stegun, *Handbook of Mathematical Functions*. New York, NY, USA: Dover, 1965.

[40] T. Riihonen, S. Werner, and R. Wichman, "Comparison of full-duplex and half-duplex modes with a fixed amplify-and-forward relay," in *Proc. IEEE WCNC*, Apr. 2009, pp. 1–5.

[41] S. Jin, M. R. McKay, X. Gao, and I. B. Collings, "Asymptotic SER and outage probability of MIMO MRC in correlated fading," *IEEE Signal Process. Lett.*, vol. 14, no. 1, pp. 9–12, Jan. 2007.

[42] A. M. Mathai, *The H-Function With Applications in Statistics and Other Disciplines*. New York, NY, USA: Wiley, 1978.

[43] K. A. Hamdi, "Capacity of MRC on correlated Rician fading channels," *IEEE Trans. Commun.*, vol. 56, no. 5, pp. 708–711, May 2008.

Ahmed Almradi received the B.Sc. degree in electrical and electronic engineering from the University of Tripoli, Tripoli, Libya, in 2004, and the M.Sc. degree in electrical and electronic engineering from the Rochester Institute of Technology, Rochester, NY, USA, in 2012, and the Ph.D. degree in electrical and electronic engineering from The University of Manchester, Manchester, U.K., in 2017. He is currently a Research Fellow with the 5G Innovation Centre, Institute for Communication Systems, University of Surrey. His research interests are in the modeling, design, and performance analysis of wireless communication systems with special emphasis on multiple-input multiple-output (MIMO) half-duplex and full-duplex relaying systems, wireless information and power transfer (energy harvesting) systems, massive MIMO millimeter-wave hybrid (analog and digital) beamforming, blind signal-to-noise ratio estimation, and OFDM systems.

Pei Xiao (SM'11) was with Newcastle University and Queen's University Belfast. He also held positions with Nokia Networks, Finland. He is currently a Professor of wireless communications with the 5G Innovation Centre (5GIC), Institute for Communication Systems, University of Surrey. He is the Technical Manager of 5GIC, leading the Research Team in the new physical layer work area and coordinating/supervising research activities across all the work areas within 5GIC (www.surrey.ac.uk/5gic/research). His technical expertise and research interests are in the fields of communication theory and signal processing for wireless communications.

Khairi Ashour Hamdi (M'99–SM'02) received the B.Sc. degree in electrical engineering from the University of Tripoli, Tripoli, Libya, in 1981, the Ph.D. degree in telecommunication engineering from the Hungarian Academy of Sciences, Budapest, Hungary, in 1993, and the M.Sc. degree (Hons.) from the Technical University of Budapest, Budapest, in 1998. He was with the University of Essex, Colchester, U.K. He is currently with the School of Electrical and Electronic Engineering, The University of Manchester, Manchester, U.K. His current research interests include modeling and performance analysis of wireless communication systems and networks, green communication systems, and heterogeneous mobile networks.